Commun. Comput. Phys.
doi: 10.4208/cicp.OA-2018-0194

Vol. **26**, No. 3, pp. 809-837
September 2019

Numerical Solution of an Inverse Obstacle Scattering Problem for Elastic Waves via the Helmholtz Decomposition

Junhong Yue[1], Ming Li[1,*], Peijun Li[2] and Xiaokai Yuan[2]

[1] *College of Data Science, Taiyuan University of Technology, Taiyuan, Shanxi 030024, P.R. China.*
[2] *Department of Mathematics, Purdue University, West Lafayette, Indiana 47907, USA.*

Received 31 July 2018; Accepted (in revised version) 22 October 2018

Abstract. Consider an inverse obstacle scattering problem in an open space which is filled with a homogeneous and isotropic elastic medium. The inverse problem is to determine the obstacle's surface from the measurement of the displacement on an artificial boundary enclosing the obstacle. In this paper, a new approach is proposed for numerical solution of the inverse problem. By introducing two scalar potential functions, the method uses the Helmholtz decomposition to split the displacement of the elastic wave equation into the compressional and shear waves, which satisfy a coupled boundary value problem of the Helmholtz equations. The domain derivative is studied for the coupled Helmholtz system. In particular, we show that the domain derivative of the potentials is the Helmholtz decomposition of the domain derivative of the displacement for the elastic wave equation. Numerical results are presented to demonstrate the effectiveness of the proposed method.

AMS subject classifications: 78A46, 65N21

Key words: The elastic wave equation, inverse obstacle scattering, domain derivative, the Helmholtz decomposition.

1 Introduction

As one of the fundamental problems in scattering theory, the obstacle scattering problem is concerned with the effect that an impenetrable medium on an incident field. If the total field is viewed as the sum of an incident field and a scattered field, the direct obstacle scattering problem is to determine the scattered field from the incident field and

*Corresponding author. *Email addresses:* `woyuejunhong@163.com` (J. Yue), `liming01@tyut.edu.cn` (M. Li), `lipeijun@math.purdue.edu` (P. Li), `yuan170@math.purdue.edu` (X. Yuan)

 ©2019 Global-Science Press

the governing equation for the wave motion; the inverse obstacle scattering problem is to determine the shape of the medium from the measurement of the scattered field. These problems have played essential roles in many scientific areas, such as radar and sonar, nondestructive testing, medical imaging, and geophysical exploration.

Driven by significant applications, the direct and inverse obstacle scattering problems have been widely studied by numerous researchers for all the three commonly encountered wave models, which include the Helmholtz equation (acoustic waves), the Maxwell equations (electromagnetic waves), and the Navier equation (elastic waves). The inverse obstacle scattering problems are challenging due to nonlinearity and ill-posedness. Computational approaches can be broadly classified into two types: optimization based iterative methods and imaging based direct methods [8, 10]. The former are named as quantitative methods while the latter are referred to as qualitative methods. The iterative methods require good initial guesses and are computationally expensive as a sequence of direct and adjoint problems need to be solved at each step of iterations. The direct methods require no a priori information on the obstacles and are computationally efficient, but the reconstructions may not be as accurate as those by using iterative methods.

For the optimization based methods, it is inevitable to calculate the domain or Fréchet derivatives when applying linearization procedures for these nonlinear problems. The domain or Fréchet derivatives characterize the variation of wave field with respect to perturbation of media such as the boundary of the obstacle. The domain derivatives have been studied by many authors for the inverse acoustic and electromagnetic obstacle scattering problems. In [32], Roger investigated the differentiability of the far-field pattern with respect to the obstacle's boundary and employed the Newton–Kantorovitch iterative method to solve the inverse obstacle scattering problem. The Fréchet derivatives of the scattering operators were studied in [12,15,19] by using the variational approaches and in [28,29] by using the boundary integral equation techniques for either the Dirichlet, Neumann, or impedance boundary condition. Recently, some related numerical results can be found in [33] on profile reconstruction for a periodic transmission problem from single-sided data.

The scattering problems for elastic waves have continuously attracted much attention by many researchers due to their significant applications in such areas as geophysics and seismology [1, 6, 21, 27]. Elastic waves are governed by the Navier equation which is complex due to the coexistence of compressional and shear waves that propagate at different speeds. In [11, 13], Hahner and Hsiao, and Elschner and Yamamoto considered the uniqueness of the inverse elastic scattering problem, separately. Various numerical methods can be found in [2, 17, 25]. The Fréchet differentiability of the boundary integral operators was studied in [7]. In [22, 23], Louër investigated domain derivatives of the inverse obstacle scattering problem for elastic waves by using the boundary integral equation method. The domain derivatives were considered in [24, 26] for the two- and three-dimensional inverse elastic obstacle scattering problems by using the variational method, and a frequency recursive method was developed to reconstruct the surface of the obstacle. Related numerical results can be found in [4, 5, 9, 31] on solving the inverse

scattering problems with multi-frequencies. A topical review can be found in [3] on the inverse source problems as well as other inverse scattering problems by using multiple frequencies to overcome the ill-posedness and gain increased stability. General references on inverse scattering problems for elastic waves may be found in [6,16,18,20,27].

In this paper, we propose a new approach to solve the inverse elastic obstacle scattering problem. The obstacle is assumed to be an elastically rigid body which is enclosed in an open space filled with a homogeneous and isotropic elastic medium. Using the Helmholtz decomposition, we introduce two scalar potential functions and split the displacement of the wave field into the compressional wave and the shear wave. Based on the transparent boundary conditions, the boundary value problem of the Navier equation is converted equivalently into a coupled boundary value problem of the Helmholtz equations for the potential functions. The purpose of this work is threefold:

1. Calculate the domain derivative of the coupled boundary value problem of the Helmholtz equations for the potential functions.

2. Establish the relation between the domain derivative of the Helmholtz system and the Helmholtz decomposition of the domain derivative for the Navier system.

3. Develop a frequency recursive method for the coupled Helmholtz system to reconstruct the obstacle's surface.

Specifically, we present a variational approach and give an explicit characterization of the domain derivative for the coupled Helmholtz system. The domain derivative is shown to be the unique weak solution of some boundary value problem which shares essentially the same variational formulation as the direct scattering problem. Hence the domain derivative can be efficiently computed by solving a direct problem. In particular, we prove that the domain derivative of the coupled Helmholtz system for the potential functions is the Helmholtz decomposition of the domain derivative of the original Navier system for the displacement. Computationally, we develop a recursive method for the inverse scattering problem. The method requires multi-frequency scattering data and proceeds from low to high frequencies. At each frequency, the steepest descent method is applied for the linearization procedure and the starting point is always taken from the output generated from the previous low frequency step. Therefore the method can create a better approximation to the surface filtered at each step of higher frequency. Numerical results demonstrate that the method is effective and stable. We mention that the proposed method is efficient as it needs only to solve the scalar Helmholtz equations and avoids solving the vector Navier equations. It provides a viable and simple alternative to solve the inverse obstacle scattering problem for elastic waves.

The rest of the paper is organized as follows. In Section 2, we introduce the model problems of the Navier equation and the coupled Helmholtz equations. The reduced boundary value problems for both the Naiver system and the Helmholtz system are presented by using the transparent boundary conditions in Section 3. Section 4 is devoted to the discussions of the domain derivatives of both systems. The recursive method is

described to solve the inverse problem in Section 5. Numerical experiments are shown to demonstrate the performance of the proposed method in Section 6. The paper is concluded with some general remarks in Section 7.

2 Problem formulation

Consider the scattering problem by a two-dimensional elastically rigid obstacle, where the obstacle is described as a bounded domain D with Lipschitz continuous boundary ∂D. Denote by $\boldsymbol{\nu}=(\nu_1,\nu_2)^\top$ and $\boldsymbol{\tau}=(\tau_1,\tau_2)^\top$ the unit normal and tangential vectors on ∂D, where $\tau_1=-\nu_2$ and $\tau_2=\nu_1$. Assume that the exterior domain $\mathbb{R}^2\backslash\overline{D}$ is filled with a homogeneous and isotropic elastic medium with a unit mass density. Denote by $B=\{x\in\mathbb{R}^2:|x|<R\}$ the disk with radius $R>0$ such that $\overline{D}\subset B$. Let $\Omega=B\backslash\overline{D}$ be the bounded domain enclosed by ∂D and ∂B. The problem geometry is shown in Fig. 1.

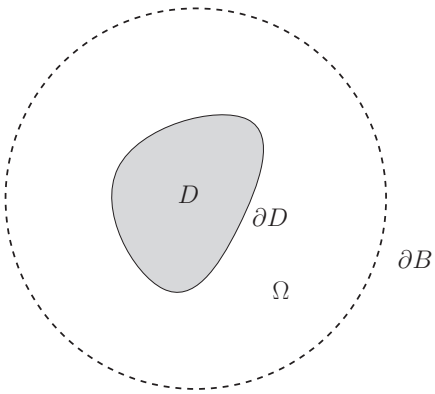

Figure 1: Problem geometry of the elastic scattering by an obstacle.

Let the obstacle be illuminated by a time-harmonic plane wave $\boldsymbol{u}^{\rm inc}$, which satisfies the two-dimensional Navier equation:

$$\mu\Delta\boldsymbol{u}^{\rm inc}+(\lambda+\mu)\nabla\nabla\cdot\boldsymbol{u}^{\rm inc}+\omega^2\boldsymbol{u}^{\rm inc}=0 \quad \text{in } \mathbb{R}^2\backslash\overline{D},$$

where $\omega>0$ is the angular frequency and λ,μ are the Lamé parameters satisfying $\mu>0$ and $\lambda+\mu>0$. More explicitly, the incident wave can be the compressional plane wave

$$\boldsymbol{u}^{\rm inc}(x)=de^{{\rm i}\kappa_1 d\cdot x},$$

or the shear plane wave

$$\boldsymbol{u}^{\rm inc}(x)=d^\perp e^{{\rm i}\kappa_2 d\cdot x},$$

or a combination of both plane waves, where $d=(\cos\theta,\sin\theta)^\top$ is the unit propagation direction vector, $\theta\in[0,2\pi)$ is the incident angle, $d^\top=(-\sin\theta,\cos\theta)^\top$ is an orthonormal vector of d, and

$$\kappa_1=\frac{\omega}{\sqrt{\lambda+2\mu}},\quad \kappa_2=\frac{\omega}{\sqrt{\mu}}$$

are the compressional wavenumber and the shear wavenumber, respectively.

The displacement of the total field $\boldsymbol{u}$ also satisfies the Navier equation:

$$\mu\Delta\boldsymbol{u}+(\lambda+\mu)\nabla\nabla\cdot\boldsymbol{u}+\omega^2\boldsymbol{u}=0 \quad \text{in } \mathbb{R}^2\backslash\overline{D}.$$

Since the obstacle is elastically rigid, $\boldsymbol{u}$ satisfies the homogeneous Dirichlet boundary condition

$$\boldsymbol{u}=0 \quad \text{on } \partial D.$$

Let the scattered field $\boldsymbol{v}=\boldsymbol{u}-\boldsymbol{u}^{\text{inc}}$. Then, $\boldsymbol{v}$ satisfies

$$\begin{cases} \mu\Delta\boldsymbol{v}+(\lambda+\mu)\nabla\nabla\cdot\boldsymbol{v}+\omega^2\boldsymbol{v}=0 & \text{in } \mathbb{R}^2\backslash\overline{D}, \\ \boldsymbol{v}=-\boldsymbol{u}^{\text{inc}} & \text{on } \partial D. \end{cases} \tag{2.1}$$

Given a vector function $\boldsymbol{v}=(v_1,v_2)^\top$ and a scalar function v, define the scalar curl operator and vector curl operator:

$$\text{curl}\boldsymbol{v}=\partial_{x_1}v_2-\partial_{x_2}v_1, \quad \mathbf{curl}v=(\partial_{x_2}v,-\partial_{x_1}v)^\top.$$

Let

$$\boldsymbol{v}_{\text{p}}=-\frac{1}{\kappa_1^2}\nabla\nabla\cdot\boldsymbol{v}, \quad \boldsymbol{v}_{\text{s}}=\frac{1}{\kappa_2^2}\mathbf{curl}\text{curl}\boldsymbol{v},$$

which are known as the compressional and shear wave components of $\boldsymbol{v}$, respectively. Since the scattering problem is imposed in the open domain $\mathbb{R}^2\backslash\overline{D}$, the scattered wave $\boldsymbol{v}$ is required to satisfy the Kupradze–Sommerfeld radiation condition [30]:

$$\lim_{\rho\to\infty}\rho^{1/2}(\partial_\rho\boldsymbol{v}_{\text{p}}-\text{i}\kappa_1\boldsymbol{v}_{\text{p}})=0, \quad \lim_{\rho\to\infty}\rho^{1/2}(\partial_\rho\boldsymbol{v}_{\text{s}}-\text{i}\kappa_2\boldsymbol{v}_{\text{s}})=0, \quad \rho=|x|.$$

For any solution $\boldsymbol{v}$ of the elastic wave equation (2.1), the Helmholtz decomposition reads

$$\boldsymbol{v}=\nabla\phi_1+\mathbf{curl}\phi_2, \tag{2.2}$$

where ϕ_j, $j=1,2$ are scalar potential functions. Substituting (2.2) into the elastic wave equation (2.1) gives

$$\nabla[(\lambda+2\mu)\Delta\phi_1+\omega^2\phi_1]+\mathbf{curl}(\mu\Delta\phi_2+\omega^2\phi_2)=0,$$

which is fulfilled if ϕ_j satisfies the Helmholtz equation

$$\Delta\phi_j+\kappa_j^2\phi_j=0.$$

In addition, ϕ_j is required to satisfy the Sommerfeld radiation condition

$$\lim_{\rho\to\infty}\rho^{1/2}(\partial_\rho\phi_j-\text{i}\kappa_j\phi_j)=0, \quad \rho=|x|. \tag{2.3}$$

It follows from the homogeneous Dirichlet boundary condition on ∂D that

$$\boldsymbol{v}=\nabla\phi_1+\mathbf{curl}\phi_2=-\boldsymbol{u}^{\rm inc}\quad \text{on } \partial D.$$

Taking the dot product of the above equation with $\boldsymbol{\nu}$ and $-\boldsymbol{\tau}$, respectively, we get

$$\partial_\nu\phi_1+\partial_\tau\phi_2=f_1,\quad \partial_\nu\phi_2-\partial_\tau\phi_1=f_2,$$

where

$$f_1=-\boldsymbol{\nu}\cdot\boldsymbol{u}^{\rm inc},\quad f_2=\boldsymbol{\tau}\cdot\boldsymbol{u}^{\rm inc}.$$

In summary, the scalar potential functions ϕ_1,ϕ_2 satisfy the coupled boundary value problem

$$\begin{cases}\Delta\phi_j+\kappa_j^2\phi_j=0 & \text{in } \mathbb{R}^2\backslash\overline{D},\\ \partial_\nu\phi_1+\partial_\tau\phi_2=f_1,\quad \partial_\nu\phi_2-\partial_\tau\phi_1=f_2 & \text{on } \partial D,\\ \lim_{\rho\to\infty}\rho^{1/2}(\partial_\rho\phi_j-{\rm i}\kappa_j\phi_j)=0, & \rho=|x|.\end{cases}\tag{2.4}$$

Let $L^2(\Omega)^2=L^2(\Omega)\times L^2(\Omega)$ be the product space of $L^2(\Omega)$ equipped with the inner product and norm:

$$(\boldsymbol{u},\boldsymbol{v})=\int_\Omega \boldsymbol{u}\cdot\bar{\boldsymbol{v}},\quad ||\boldsymbol{u}||_{0,\Omega}=(\boldsymbol{u},\boldsymbol{u})^{1/2}.$$

Let $H^s(\Omega)$ and $H^s(\partial B)$ be the standard Sobolev spaces with the norms given by

$$||w||_{s,\Omega}^2=\sum_{|\alpha|\le s}\int_\Omega |D^\alpha w|^2$$

and

$$||w||_{s,\partial B}^2=2\pi\sum_{n\in\mathbb{Z}}(1+n^2)^s|w^{(n)}(R)|^2,$$

where $w^{(n)}(R),n\in\mathbb{Z}$ are the Fourier coefficients of w on ∂B_R, i.e.,

$$w^{(n)}(R)=\frac{1}{2\pi}\int_0^{2\pi} w(R,\theta)e^{-{\rm i}n\theta}{\rm d}\theta.$$

Define $H^1_{\partial D}(\Omega)=\{w\in H^1(\Omega):w=0 \text{ on } \partial D\}$. Let $H^1_{\partial D}(\Omega)^2=H^1_{\partial D}(\Omega)\times H^1_{\partial D}(\Omega)$ and $H^s(\partial B)^2=H^s(\partial B)\times H^s(\partial B)$ be the Cartesian product spaces equipped with the corresponding 2-norms of $H^1_{\partial D}(\Omega)$ and $H^s(\partial B)$, respectively. It is known that $H^{-s}(\partial B)^2$ is the dual space of $H^s(\partial B)^2$ with respect to the inner product

$$\langle\boldsymbol{u},\boldsymbol{v}\rangle_{\partial B}=\int_{\partial B}\boldsymbol{u}\cdot\bar{\boldsymbol{v}}.$$

3 Reduced problems

In this section, we introduce the transparent boundary conditions on ∂B to reduce equivalently the boundary value problems (2.1) and (2.4) into the bounded domain Ω.

In the exterior domain $\mathbb{R}^2\backslash\overline{B}$, it follows from the radiation condition (2.3) that the solutions of (2.4) have the Fourier series expansions in the polar coordinates

$$\phi_j(\rho,\theta)=\sum_{n\in\mathbb{Z}}\frac{H_n^{(1)}(\kappa_j\rho)}{H_n^{(1)}(\kappa_j R)}\phi_j^{(n)}(R)e^{\mathrm{i}n\theta}, \tag{3.1}$$

where $H_n^{(1)}$ is the Hankel function of the first kind with order n.

For a given function w on ∂B, it has the Fourier series expansion

$$w(R,\theta)=\sum_{n\in\mathbb{Z}}w^{(n)}e^{in\theta},\quad w^{(n)}=\frac{1}{2\pi}\int_0^{2\pi}w(R,\theta)e^{-\mathrm{i}n\theta}\mathrm{d}\theta.$$

We define two boundary operators

$$(\mathscr{T}_j w)(R,\theta)=\frac{1}{R}\sum_{n\in\mathbb{Z}}h_n(\kappa_j R)w^{(n)}e^{\mathrm{i}n\theta}, \tag{3.2}$$

where $h_n(z)=zH_n^{(1)'}(z)/H_n^{(1)}(z)$. Taking the derivative of (3.1) with respect to ρ, evaluating it at $\rho=R$, and using the boundary operators (3.2), we get the transparent boundary condition

$$\partial_\rho\phi_j=\mathscr{T}_j\phi_j\quad\text{on }\partial B. \tag{3.3}$$

In the frequency domain, the transparent boundary condition (3.3) becomes

$$(\partial_\rho\phi_j)^{(n)}(R)=\alpha_j^{(n)}\phi_j^{(n)}(R),\quad \alpha_j^{(n)}=\frac{\kappa_j H_n^{(1)'}(\kappa_j R)}{H_n^{(1)}(\kappa_j R)}. \tag{3.4}$$

Taking $\partial_{\rho\rho}$ of (3.1) and then evaluating it at $\rho=R$ yields

$$(\partial_{\rho\rho}\phi_j)^{(n)}(R)=\beta_j^{(n)}\phi_j^{(n)}(R),\quad \beta_j^{(n)}=\frac{\kappa_j^2 H_n^{(1)''}(\kappa_j R)}{H_n^{(1)}(\kappa_j R)}. \tag{3.5}$$

The polar coordinates (ρ,θ) are related to the Cartesian coordinates $\boldsymbol{x}=(x_1,x_2)^\top$ by $x_1=\rho\cos\theta, x_2=\rho\sin\theta$. The local orthonormal basis is

$$\boldsymbol{e}_\rho=(\cos\theta,\sin\theta)^\top,\quad \boldsymbol{e}_\theta=(-\sin\theta,\cos\theta)^\top.$$

For any vector $\boldsymbol{w}=(w_1,w_2)^\top$ given in the Cartesian coordinates, it has a representation in the polar coordinates $\boldsymbol{w}=\hat{w}_1\boldsymbol{e}_\rho+\hat{w}_2\boldsymbol{e}_\theta$, which will be still denoted as $\boldsymbol{w}=(\hat{w}_1,\hat{w}_2)^\top$ for simplicity. For any function w, it is easy to verify that

$$\nabla w=\left(\partial_\rho w,\frac{1}{\rho}\partial_\theta w\right)^\top,\quad \mathbf{curl}w=\left(\frac{1}{\rho}\partial_\theta w,-\partial_\rho w\right)^\top,$$

and

$$\Delta w=\left(\partial_{\rho\rho}+\frac{1}{\rho}\partial_\rho+\frac{1}{\rho^2}\partial_{\theta\theta}\right)w.$$

In the new coordinates, the Helmholtz decomposition (2.2) takes the form

$$\boldsymbol{v}=\left(\partial_\rho\phi_1+\frac{1}{\rho}\partial_\theta\phi_2,\frac{1}{\rho}\partial_\theta\phi_1-\partial_\rho\phi_2\right)^\top. \tag{3.6}$$

Taking the Fourier transform of (3.6) at $\rho=R$ and applying the boundary condition (3.4), we obtain

$$\boldsymbol{v}^{(n)}(R)=\begin{bmatrix}\alpha_1^{(n)} & \frac{\mathrm{i}n}{R}\\ \frac{\mathrm{i}n}{R} & -\alpha_2^{(n)}\end{bmatrix}\begin{bmatrix}\phi_1^{(n)}(R)\\ \phi_2^{(n)}(R)\end{bmatrix}. \tag{3.7}$$

Taking ∂_ρ of (3.6), applying the Fourier transform, and using (3.4)-(3.5), we have

$$(\partial_\rho\boldsymbol{v})^{(n)}(R)=\begin{bmatrix}\beta_1^{(n)} & -\frac{\mathrm{i}n}{R^2}+\frac{\mathrm{i}n}{R}\alpha_2^{(n)}\\ -\frac{\mathrm{i}n}{R^2}+\frac{\mathrm{i}n}{R}\alpha_1^{(n)} & -\beta_2^{(n)}\end{bmatrix}\begin{bmatrix}\phi_1^{(n)}(R)\\ \phi_2^{(n)}(R)\end{bmatrix}. \tag{3.8}$$

It follows from (2.2) that

$$\nabla\cdot\boldsymbol{v}=\Delta\phi_1=\left(\partial_{\rho\rho}+\frac{1}{\rho}\partial_\rho+\frac{1}{\rho^2}\partial_{\theta\theta}\right)\phi_1,$$

which yields after taking the Fourier transform that

$$(\nabla\cdot\boldsymbol{v})^{(n)}(R)=\left(\beta_1^{(n)}+\frac{1}{R}\alpha_1^{(n)}-\left(\frac{n}{R}\right)^2\right)\phi_1^{(n)}(R). \tag{3.9}$$

Define a boundary operator for the displacement of the scattered wave

$$\mathscr{B}\boldsymbol{v}=\mu\partial_\rho\boldsymbol{v}+(\lambda+\mu)(\nabla\cdot\boldsymbol{v})\boldsymbol{e}_\rho\quad\text{on }\partial B,$$

which gives after taking the Fourier transform and using (3.8)-(3.9) that

$$\begin{aligned}(\mathscr{B}\boldsymbol{v})^{(n)}(R)=&\,\mu\begin{bmatrix}\beta_1^{(n)} & -\frac{\mathrm{i}n}{R^2}+\frac{\mathrm{i}n}{R}\alpha_2^{(n)}\\ -\frac{\mathrm{i}n}{R^2}+\frac{\mathrm{i}n}{R}\alpha_1^{(n)} & -\beta_2^{(n)}\end{bmatrix}\begin{bmatrix}\phi_1^{(n)}(R)\\ \phi_2^{(n)}(R)\end{bmatrix}\\ &+(\lambda+\mu)\begin{bmatrix}\beta_1^{(n)}+\frac{1}{R}\alpha_1^{(n)}-\frac{n^2}{R^2} & 0\\ 0 & 0\end{bmatrix}\begin{bmatrix}\phi_1^{(n)}(R)\\ \phi_2^{(n)}(R)\end{bmatrix}.\end{aligned} \tag{3.10}$$

Combining (3.7) and (3.10) yields the transparent boundary condition:

$$\mathscr{B}\boldsymbol{v}=\mathscr{T}\boldsymbol{v}:=\sum_{n\in\mathbb{Z}}M_n\boldsymbol{v}^{(n)}e^{\mathrm{i}n\theta}\quad\text{on }\partial B, \tag{3.11}$$

where

$$M_n=\begin{bmatrix}M_{11}^{(n)} & M_{12}^{(n)}\\ M_{21}^{(n)} & M_{22}^{(n)}\end{bmatrix}=\Lambda_n^{-1}\begin{bmatrix}N_{11}^{(n)} & N_{12}^{(n)}\\ N_{21}^{(n)} & N_{22}^{(n)}\end{bmatrix}.$$

Here

$$\Lambda_n=\left(\frac{n}{R}\right)^2-\alpha_1^{(n)}\alpha_2^{(n)}$$

and

$$N_{11}^{(n)}=-\alpha_2^{(n)}\xi^{(n)}+\mu\left(\frac{n}{R}\right)^2\eta_2^{(n)},\quad N_{12}^{(n)}=-\frac{\mathrm{i}n}{R}\xi^{(n)}+\mu\frac{\mathrm{i}n}{R}\alpha_1^{(n)}\eta_2^{(n)},$$

$$N_{21}^{(n)}=-\mu\frac{\mathrm{i}n}{R}\alpha_2^{(n)}\eta_1^{(n)}+\mu\frac{\mathrm{i}n}{R}\beta_2^{(n)},\quad N_{22}^{(n)}=\mu\left(\frac{n}{R}\right)^2\eta_1^{(n)}-\mu\alpha_1^{(n)}\beta_2^{(n)},$$

where

$$\xi^{(n)}=(\lambda+2\mu)\beta_1^{(n)}+(\lambda+\mu)\left(\frac{1}{R}\alpha_1^{(n)}-\left(\frac{n}{R}\right)^2\right),\quad \eta_j^{(n)}=\alpha_j^{(n)}-\frac{1}{R}.$$

Using the transparent boundary condition (3.11), we can reformulate the scattering problem to the following boundary value problem

$$\begin{cases}\mu\Delta\boldsymbol{u}+(\lambda+\mu)\nabla\nabla\cdot\boldsymbol{u}+\omega^2\boldsymbol{u}=0 & \text{in }\Omega,\\ \boldsymbol{u}=0 & \text{on }\partial D,\\ \mathscr{B}\boldsymbol{u}=\mathscr{T}\boldsymbol{u}+\boldsymbol{g} & \text{on }\partial B,\end{cases} \tag{3.12}$$

where $\boldsymbol{g}=(\mathscr{B}-\mathscr{T})\boldsymbol{u}^{\mathrm{inc}}$. The variational problem of (3.12) is to find $\boldsymbol{u}\in H^1_{\partial D}(\Omega)^2$ such that

$$b(\boldsymbol{u},\boldsymbol{v})=\langle\boldsymbol{g},\boldsymbol{v}\rangle_{\partial B},\quad\forall\boldsymbol{v}\in H^1_{\partial D}(\Omega)^2,$$

where the sesquilinear form $b:H^1_{\partial D}(\Omega)^2\times H^1_{\partial D}(\Omega)^2\to\mathbb{C}$ is defined by

$$b(\boldsymbol{u},\boldsymbol{v})=\mu\int_\Omega\nabla\boldsymbol{u}:\nabla\bar{\boldsymbol{v}}+(\lambda+\mu)\int_\Omega(\nabla\cdot\boldsymbol{u})(\nabla\cdot\bar{\boldsymbol{v}})-\omega^2\int_\Omega\boldsymbol{u}\cdot\bar{\boldsymbol{v}}-\langle\mathscr{T}\boldsymbol{u},\boldsymbol{v}\rangle_{\partial B}. \tag{3.13}$$

Here $A:B=\mathrm{tr}(AB^\top)$ is the Frobenius inner product of square matrices A,B.

Alternatively, using the transparent boundary conditions (3.3), the coupled system (2.4) can also be reformulated into a coupled boundary value problem

$$\begin{cases}\Delta\phi_j+\kappa_j^2\phi_j=0 & & \text{in }\Omega,\\ \partial_\nu\phi_1+\partial_\tau\phi_2=f_1, & \partial_\nu\phi_2-\partial_\tau\phi_1=f_2 & \text{on }\partial D,\\ \partial_\rho\phi_j-\mathscr{T}_j\phi_j=0 & & \text{on }\partial B.\end{cases} \tag{3.14}$$

The weak formulation of (3.14) is to find $(\phi_1,\phi_2)\in H^1(\Omega)^2$ such that

$$a(\phi_1,\phi_2;\psi_1,\psi_2)=-\sum_{j=1}^{2}\langle f_j,\psi_j\rangle_{\partial D},\quad \forall(\psi_1,\psi_2)\in H^1(\Omega)^2,$$

where the sesquilinear form $a:H^1(\Omega)^2\times H^1(\Omega)^2\to\mathbb{C}$ is defined by

$$\begin{aligned}a(\phi_1,\phi_2;\psi_1,\psi_2)=&\sum_{j=1}^{2}\int_\Omega\nabla\phi_j\cdot\nabla\bar{\psi}_j-\kappa_j^2\int_\Omega\phi_j\bar{\psi}_j-\langle\mathscr{T}_j\phi_j,\psi_j\rangle_{\partial B}\\&-\int_{\partial D}\partial_\tau\phi_2\bar{\psi}_1+\int_{\partial D}\partial_\tau\phi_1\bar{\psi}_2.\end{aligned}\tag{3.15}$$

We may also consider the Helmholtz decomposition for total field $\boldsymbol{u}$:

$$\boldsymbol{u}=\nabla\varphi_1+\mathbf{curl}\varphi_2.$$

It is easy to verify that φ_1,φ_2 satisfy

$$\begin{cases}\Delta\varphi_j+\kappa_j^2\varphi_j=0 & \text{in }\Omega,\\ \partial_\nu\varphi_1+\partial_\tau\varphi_2=0,\quad \partial_\nu\varphi_2-\partial_\tau\varphi_1=0 & \text{on }\partial D,\\ \partial_\rho\varphi_j-\mathscr{T}_j\varphi_j=g_j & \text{on }\partial B,\end{cases}\tag{3.16}$$

where $g_j=\partial_\rho\phi_j^{\rm inc}-\mathscr{T}_j\phi_j^{\rm inc}$ and

$$\phi_1^{\rm inc}=-\frac{1}{\kappa_1^2}\nabla\cdot\boldsymbol{u}^{\rm inc},\quad \phi_2^{\rm inc}=\frac{1}{\kappa_2^2}{\rm curl}\boldsymbol{u}^{\rm inc}.$$

The variational form of problem (3.16) is to find $(\varphi_1,\varphi_2)\in H^1(\Omega)^2$ such that

$$a(\varphi_1,\varphi_2;\psi_1,\psi_2)=\sum_{j=1}^{2}\langle g_j,\psi_j\rangle_{\partial B},\quad \forall(\psi_1,\psi_2)\in H^1(\Omega)^2.\tag{3.17}$$

We refer to [24] for the proofs of the well-posedness of the boundary value problems (3.12), (3.14), and (3.16).

4 Domain derivatives

In this section, we study the domain derivatives for the boundary value problems (3.12) and (3.16). Then we show that the Helmholtz decomposition of the domain derivative of (3.12) is just the domain derivative of (3.16).

4.1 Domain derivative for Navier equation

Given $h>0$, introduce a domain Ω_h enclosed by ∂D_h and ∂B, where

$$\partial D_h=\{\boldsymbol{x}+h\boldsymbol{p}(\boldsymbol{x}):\boldsymbol{x}\in\partial D\},$$

where the obstacle's surface ∂D is assumed to be in C^2 and the function $\boldsymbol{p}\in C^2(\partial D)^2$. It is clear to note that $\partial D_h\in C^2$ is a perturbation of ∂D for sufficiently small h.

Let $\boldsymbol{u}_h$ be the solution of the boundary value problem (3.12) for Navier equation corresponding to the domain Ω_h. Define a nonlinear scattering operator

$$\mathscr{S}:\partial D_h\to\gamma\boldsymbol{u}_h,$$

where γ is the trace operator onto ∂B. The domain derivative of the operator $\mathscr{S}$ on the boundary ∂D along with the direction $\boldsymbol{p}$ is defined by

$$\mathscr{S}'(\partial D,\boldsymbol{p}):=\lim_{h\to 0}\frac{\mathscr{S}(\partial D_h)-\mathscr{S}(\partial D)}{h}=\lim_{h\to 0}\frac{\gamma\boldsymbol{u}_h-\gamma\boldsymbol{u}}{h}.$$

The following result on the domain derivative of (3.12) is proved in [24].

Theorem 4.1. *Let $\boldsymbol{u}$ be the solution of the variational problem* (3.13). *Given $\boldsymbol{p}\in C^2(\partial D)^2$, the domain derivative of the scattering operator $\mathscr{S}$ is $\mathscr{S}'(\partial D;\boldsymbol{p})=\gamma\boldsymbol{u}'$, where $\boldsymbol{u}'$ is the unique weak solution of the boundary value problem:*

$$\begin{cases}\mu\Delta\boldsymbol{u}'+(\lambda+\mu)\nabla\nabla\cdot\boldsymbol{u}'+\omega^2\boldsymbol{u}'=0 & \text{in } \Omega,\\ \boldsymbol{u}'=-(\boldsymbol{p}\cdot\boldsymbol{\nu})\partial_\nu\boldsymbol{u} & \text{on } \partial D,\\ \mathscr{B}\boldsymbol{u}'=\mathscr{T}\boldsymbol{u}' & \text{on } \partial B.\end{cases}\tag{4.1}$$

4.2 Domain derivative for the coupled Helmholtz system

Consider the variational problem of the coupled Helmholtz system (3.16) in the perturbed domain $\Omega_h=B\backslash\overline{D}_h$: to find $(\varphi_1^h,\varphi_2^h)\in H^1(\Omega)^2$ such that

$$a_h(\varphi_1^h,\varphi_2^h;\psi_1^h,\psi_2^h)=\sum_{j=1}^{2}\langle g_j,\psi_j^h\rangle_{\partial B},\quad\forall(\psi_1^h,\psi_2^h)\in H^1(\Omega_h)^2,\tag{4.2}$$

where the sesquilinear form

$$\begin{aligned}a_h(\varphi_1^h,\varphi_2^h;\psi_1^h,\psi_2^h)=&\sum_{j=1}^{2}\int_{\Omega_h}\nabla\varphi_j^h\cdot\nabla\bar{\psi}_j^h-\kappa_j^2\int_{\Omega_h}\varphi_j^h\bar{\psi}_j^h-\langle\mathscr{T}_j\varphi_j^h,\psi_j^h\rangle_{\partial B}\\&-\int_{\partial D_h}\partial_\tau\varphi_2^h\bar{\psi}_1^h+\int_{\partial D_h}\partial_\tau\varphi_1^h\bar{\psi}_2^h.\end{aligned}$$

Define a nonlinear scattering operator for φ_j^h:

$$\mathscr{S}_j:\partial D_h\to\gamma\varphi_j^h,\quad j=1,2.$$

The domain derivative of $\mathscr{S}_j$ on the boundary ∂D along with the direction $\boldsymbol{p}$ is defined by

$$\mathscr{S}_j'(\partial D,\boldsymbol{p}):=\lim_{h\to 0}\frac{\mathscr{S}_j(\partial D_h)-\mathscr{S}_j(\partial D)}{h}=\lim_{h\to 0}\frac{\gamma\varphi_j^h-\gamma\varphi_j}{h}.$$

For a given $\boldsymbol{p}\in C^2(\partial D)^2$, we extend its domain to $\overline{\Omega}$ by requiring that $\boldsymbol{p}\in C^2(\Omega)^2\cap C(\overline{\Omega})^2$ and $\boldsymbol{p}=\boldsymbol{0}$ on ∂B. Hence $\boldsymbol{y}=\xi^h(\boldsymbol{x})=\boldsymbol{x}+h\boldsymbol{p}(\boldsymbol{x})$ maps Ω to Ω_h. It is clear to note that ξ^h is a diffemorphism from Ω to Ω_h for sufficiently small h. Denote by $\eta^h(\boldsymbol{y}):\Omega_h\to\Omega$ the inverse map of ξ^h. Define $\breve{\varphi}_j(\boldsymbol{x})=(\varphi_j^h\circ\xi^h)(\boldsymbol{x}),j=1,2$. It follows from the change of variables that we have

$$\begin{aligned}
&\int_{\Omega_h}\nabla\varphi_j^h\cdot\nabla\psi_j^h=\int_{\Omega}(\nabla\bar{\breve{\psi}}_j)^\top J_{\eta^h}J_{\eta^h}^\top\nabla\breve{\varphi}_j\det(J_{\xi^h}),\\
&\int_{\Omega_h}\varphi_j^h\bar{\psi}_j^h=\int_{\Omega}\breve{\varphi}_j\bar{\breve{\psi}}_j\det(J_{\xi^h}),\\
&\int_{\partial D_h}\partial_\tau\varphi_2^h\bar{\psi}_1^h=\int_{\partial D}\boldsymbol{\tau}_h\cdot(J_{\eta^h}^\top\nabla\breve{\varphi}_2)\bar{\breve{\psi}}_1\det(J_{\xi^h}),\\
&\int_{\partial D_h}\partial_\tau\varphi_1^h\bar{\psi}_2^h=\int_{\partial D}\boldsymbol{\tau}_h\cdot(J_{\eta^h}^\top\nabla\breve{\varphi}_1)\bar{\breve{\psi}}_2\det(J_{\xi^h}),
\end{aligned}$$

where $\boldsymbol{\tau}_h$ is the unit normal vector on ∂D_h, $\breve{\psi}_j=(\psi_j^h\circ\xi^h)(\boldsymbol{x})$, J_{η^h} and J_{ξ^h} are the Jacobian matrices of the transforms of η^h and ξ^h, respectively.

Since ψ_j^h is an arbitrary test function in the domain Ω_h, it is easy to note that $\breve{\psi}_j$ is also a test function in the domain Ω according to the transform. Hence the sesquilinear form a^h in (4.2) can be written as

$$\begin{aligned}
a^h(\breve{\varphi}_1,\breve{\varphi}_2;\psi_1,\psi_2)=&\sum_{j=1}^2\int_{\Omega}(\nabla\bar{\psi}_j)^\top J_{\eta^h}J_{\eta^h}^\top\nabla\breve{\varphi}_j\det(J_{\xi^h})-\kappa_j^2\int_{\Omega}\breve{\varphi}_j\bar{\psi}_j\det(J_{\xi^h})-\langle\mathscr{T}_j\breve{\varphi}_j,\psi_j\rangle_{\partial B}\\
&-\int_{\partial D}\boldsymbol{\tau}_h\cdot(J_{\eta^h}^\top\nabla\breve{\varphi}_2)\bar{\psi}_1\det(J_{\xi^h})+\int_{\partial D}\boldsymbol{\tau}_h\cdot(J_{\eta^h}^\top\nabla\breve{\varphi}_1)\bar{\psi}_2\det(J_{\xi^h}),
\end{aligned}\tag{4.3}$$

which gives an equivalent variational formulation of (4.2):

$$a^h(\breve{\varphi}_1,\breve{\varphi}_2;\psi_1,\psi_2)=\sum_{j=1}^2\langle g_j,\psi_j\rangle_{\partial B},\quad\forall(\psi_1,\psi_2)\in H^1(\Omega)^2.\tag{4.4}$$

Combining (3.17), (4.4), and (4.3) yields

$$\begin{aligned} a(\breve{\varphi}_1-\varphi_1,\breve{\varphi}_2-\varphi_2;\psi_1,\psi_2) &= a(\breve{\varphi}_1,\breve{\varphi}_2;\psi_1,\psi_2)-a(\varphi_1,\varphi_2;\psi_1,\psi_2) \\ &= a(\breve{\varphi}_1,\breve{\varphi}_2;\psi_1,\psi_2)-\sum_{j=1}^{2}\langle g_j,\psi_j\rangle_{\partial B} \\ &= a(\breve{\varphi}_1,\breve{\varphi}_2;\psi_1,\psi_2)-a^h(\breve{\varphi}_1,\breve{\varphi}_2;\psi_1,\psi_2). \end{aligned}$$

Hence

$$\begin{aligned} &a(\breve{\varphi}_1-\varphi_1,\breve{\varphi}_2-\varphi_2;\psi_1,\psi_2) \\ =&\sum_{j=1}^{2}\int_\Omega(\nabla\bar{\psi}_j)^\top[I-J_{\eta^h}J_{\eta^h}^\top\det(J_{\xi^h})]\nabla\breve{\varphi}_j-\kappa_j^2\int_\Omega[1-\det(J_{\xi^h})]\breve{\varphi}_j\bar{\psi}_j \\ &-\int_{\partial D}[\boldsymbol{\tau}-\det(J_{\xi^h})J_{\eta^h}\boldsymbol{\tau}_h]\cdot\nabla\breve{\varphi}_2\bar{\psi}_1+\int_{\partial D}[\boldsymbol{\tau}-\det(J_{\xi^h})J_{\eta^h}\boldsymbol{\tau}_h]\cdot\nabla\breve{\varphi}_1\bar{\psi}_2. \end{aligned} \tag{4.5}$$

Following the definitions of the Jacobian matrices, we may easily verify that

$$\begin{aligned} &\det(J_{\xi^h})=1+h\nabla\cdot\boldsymbol{p}+\mathcal{O}(h^2), \\ &J_{\eta^h}=J_{\xi^h}^{-1}\circ\eta^h=I-hJ_p+\mathcal{O}(h^2), \\ &J_{\eta^h}J_{\eta^h}^\top\det(J_{\xi^h})=I-h(J_p+J_p^\top)+h(\nabla\cdot\boldsymbol{p})I+\mathcal{O}(h^2), \end{aligned}$$

where I is the identity matrix and $J_p=\nabla\boldsymbol{p}$.

As a closed curve, the obstacle's surface has a parametric equation

$$\partial D=\{\boldsymbol{r}\in\mathbb{R}^2:\boldsymbol{r}(t)=(r_1(t),r_2(t))^\top,\ t\in[0,2\pi]\}.$$

It is easy to note that

$$\boldsymbol{\tau}=\frac{(r_1'(t),r_2'(t))^\top}{|r'(t)|},\quad \boldsymbol{\nu}=\frac{(r_2'(t),-r_1'(t))^\top}{|r'(t)|}.$$

Lemma 4.1. *Let $\boldsymbol{p}=(p_1,p_2)^\top$. Then for sufficiently small h, the following estimates hold:*

$$\begin{aligned} &\det(J_{\xi^h})=1+h[\partial_x p_1 r_1'(t)^2+\partial_y p_2 r_2'(t)^2]+h(\partial_y p_1+\partial_x p_2)r_1'(t)r_2'(t)+\mathcal{O}(h^2), \\ &\boldsymbol{\tau}_h=\boldsymbol{\tau}+hJ_p\boldsymbol{\tau}-h[\partial_x p_1 r_1'(t)^2+\partial_y p_1 r_2'(t)^2]\boldsymbol{\tau}-h(\partial_y p_1+\partial_x p_2)r_1'(t)r_2'(t)\boldsymbol{\tau}+\mathcal{O}(h^2). \end{aligned}$$

Proof. Let $\boldsymbol{r}(t),t\in[0,2\pi]$ be the parametric equation of ∂D. Then the parametric equation of ∂D_h is

$$\breve{\boldsymbol{r}}(t)=\begin{pmatrix}\breve{r}_1(t)\\ \breve{r}_2(t)\end{pmatrix}=\boldsymbol{r}(t)+h\boldsymbol{p}(r(t))=\begin{pmatrix}r_1(t)+hp_1(r_1(t),r_2(t))\\ r_2(t)+hp_2(r_1(t),r_2(t))\end{pmatrix}.$$

It follows from the straightforward calculation that

$$
\begin{aligned}
\det(J_{\tilde{\xi}^h}) &= |\check{\boldsymbol{r}}'(t)| = (\check{r}_1'(t)^2+\check{r}_2'(t)^2)^{1/2} \\
&= \big\{[r_1'(t)+h\partial_x p_1 r_1'(t)+h\partial_y p_1 r_2'(t)]^2+[r_2'(t)+h\partial_x p_2 r_1'(t)+h\partial_y p_2 r_2'(t)]^2\big\}^{1/2} \\
&= \big\{r_1'(t)^2+h^2(\partial_x p_1)^2 r_1'(t)^2+h^2(\partial_y p_1)^2 r_2'(t)^2+2h\partial_x p_1 r_1'(t)^2+2h\partial_y p_1 r_1'(t) r_2'(t) \\
&\qquad +2h^2\partial_x p_1\partial_y p_1 r_1'(t) r_2'(t)+r_2'(t)^2+h^2(\partial_x p_2)^2 r_1'(t)^2+h^2(\partial_y p_2)^2 r_2'(t)^2 \\
&\qquad +2h\partial_x p_2 r_1'(t) r_2'(t)+2h\partial_y p_2 r_2'(t)^2+2h^2\partial_x p_2\partial_y p_2 r_1'(t) r_2'(t)\big\}^{1/2} \\
&= \big\{1+h^2[(\partial_x p_1)^2+(\partial_x p_2)^2] r_1'(t)^2+h^2[(\partial_y p_1)^2+(\partial_y p_2)^2] r_2'(t)^2 \\
&\qquad +2h(\partial_x p_1 r_1'(t)^2+\partial_y p_2 r_2'(t)^2)+2h(\partial_y p_1+\partial_x p_2) r_1'(t) r_2'(t) \\
&\qquad +2h^2(\partial_x p_1\partial_y p_1+\partial_x p_2\partial_y p_2) r_1'(t) r_2'(t)\big\}^{1/2} \\
&= 1+\frac{1}{2}\big\{2h(\partial_x p_1 r_1'(t)^2+\partial_y p_2 r_2'(t)^2)+2h(\partial_y p_1+\partial_x p_2) r_1'(t) r_2'(t)\big\}+\mathcal{O}(h^2) \\
&= 1+h(\partial_x p_1 r_1'(t)^2+\partial_y p_2 r_2'(t)^2)+h(\partial_y p_1+\partial_x p_2) r_1'(t) r_2'(t)+\mathcal{O}(h^2).
\end{aligned}
$$

Let $\boldsymbol{\tau}_h$ be the unit tangent vector on ∂D_h. Then

$$
\begin{aligned}
\boldsymbol{\tau}_h &= |\check{\boldsymbol{r}}'(t)|^{-1}\begin{pmatrix}\check{r}_1'(t)\\ \check{r}_2'(t)\end{pmatrix} = |\check{\boldsymbol{r}}'(t)|^{-1}\begin{pmatrix} r_1'(t)+h\partial_x p_1 r_1'(t)+h\partial_y p_1 r_2'(t)\\ r_2'(t)+h\partial_x p_2 r_1'(t)+h\partial_y p_2 r_2'(t)\end{pmatrix} \\
&= \big[1-h(\partial_x p_1 r_1'(t)^2+\partial_y p_2 r_2'(t)^2)-h(\partial_y p_1+\partial_x p_2) r_1'(t) r_2'(t)+\mathcal{O}(h^2)\big] \\
&\qquad \times\left(\boldsymbol{\tau}+h\begin{bmatrix}\partial_x p_1 & \partial_y p_1\\ \partial_x p_2 & \partial_y p_2\end{bmatrix}\boldsymbol{\tau}\right) \\
&= \boldsymbol{\tau}+hJ_p\boldsymbol{\tau}-h(\partial_x p_1 r_1'(t)^2+\partial_y p_2 r_2'(t)^2)\boldsymbol{\tau}-h(\partial_y p_1+\partial_x p_2) r_1'(t) r_2'(t)\boldsymbol{\tau}+\mathcal{O}(h^2),
\end{aligned}
$$

which completes the proof. □

Using Lemma 4.1, we obtain

$$
\begin{aligned}
&\boldsymbol{\tau}-\det(J_{\tilde{\xi}^h})J_{\eta^h}\boldsymbol{\tau}_h \\
=&\boldsymbol{\tau}-\big(1+h[\partial_x p_1 r_1'(t)^2+\partial_y p_2 r_2'(t)^2]+h[\partial_y p_1+\partial_x p_2] r_1'(t) r_2'(t)+\mathcal{O}(h^2)\big) \\
&\quad (I-hJ_p)\big(\boldsymbol{\tau}+hJ_p\boldsymbol{\tau}-h[\partial_x p_1 r_1'(t)^2+\partial_y p_2 r_2'(t)^2]\boldsymbol{\tau}-h[\partial_y p_1+\partial_x p_2] r_1'(t) r_2'(t)\boldsymbol{\tau}+\mathcal{O}(h^2)\big) \\
=&\boldsymbol{\tau}-\big(\boldsymbol{\tau}+hJ_p\boldsymbol{\tau}-h[\partial_x p_1 r_1'(t)^2+\partial_y p_2 r_2'(t)^2]\boldsymbol{\tau}-h[\partial_y p_1+\partial_x p_2] r_1'(t) r_2'(t)\boldsymbol{\tau} \\
&\quad -hJ_p\boldsymbol{\tau}+h[\partial_x p_1 r_1'(t)^2+\partial_y p_2 r_2'(t)^2]\boldsymbol{\tau}+h[\partial_y p_1+\partial_x p_2] r_1'(t) r_2'(t)\big)\boldsymbol{\tau}+\mathcal{O}(h^2) \\
=&\mathcal{O}(h^2).
\end{aligned}
$$

Using the above estimates, we can easily verify that

$$
\begin{aligned}
&(\nabla\bar{\psi}_j)^\top[I-J_{\eta^h}J_{\eta^h}^\top\det(J_{\tilde{\xi}^h})]\nabla\check{\varphi}_j = h(\nabla\bar{\psi}_j)^\top[J_p+J_p^\top-(\nabla\cdot\boldsymbol{p})I]\nabla\check{\varphi}_j+\mathcal{O}(h^2), \\
&[1-\det(J_{\tilde{\xi}^h})]\check{\varphi}_j\bar{\psi}_j = -h(\nabla\cdot\boldsymbol{p})\check{\varphi}_j\bar{\psi}_j+\mathcal{O}(h^2),
\end{aligned}
$$

$$[\boldsymbol{\tau}-\det(J_{\tilde{\xi}^h})J_{\eta^h}\tau_h]\cdot\nabla\breve{\varphi}_2\bar{\psi}_1=\mathcal{O}(h^2),$$
$$[\boldsymbol{\tau}-\det(J_{\tilde{\xi}^h})J_{\eta^h}\tau_h]\cdot\nabla\breve{\varphi}_1^h\bar{\psi}_2=\mathcal{O}(h^2).$$

Hence, we have from (4.5) and the above estimates that

$$\begin{aligned}
&a\left(\frac{\breve{\varphi}_1^h-\varphi_1}{h},\frac{\breve{\varphi}_2^h-\varphi_2}{h};\psi_1,\psi_2\right)\\
=&\frac{1}{h}\sum_{j=1}^{2}\int_\Omega(\nabla\bar{\psi}_j)^\top[I-J_{\eta^h}J_{\eta^h}^\top\det(J_{\tilde{\xi}^h})]\nabla\breve{\varphi}_j-\kappa_j^2\int_\Omega[1-\det(J_{\tilde{\xi}^h})]\breve{\varphi}_j\bar{\psi}_j\\
&-\frac{1}{h}\int_{\partial D}[\boldsymbol{\tau}-\det(J_{\tilde{\xi}^h})J_{\eta^h}\boldsymbol{\tau}_h]\cdot\nabla\breve{\varphi}_2\bar{\psi}_1+\frac{1}{h}\int_{\partial D}[\boldsymbol{\tau}-\det(J_{\tilde{\xi}^h})J_{\eta^h}\boldsymbol{\tau}_h]\cdot\nabla\breve{\varphi}_1\bar{\psi}_2\\
=&g_1(\boldsymbol{p})(\breve{\varphi}_1,\breve{\varphi}_2;\psi_1,\psi_2)+g_2(\boldsymbol{p})(\breve{\varphi}_1,\breve{\varphi}_2;\psi_1,\psi_2)+\mathcal{O}(h),
\end{aligned}\tag{4.6}$$

where

$$g_1(\boldsymbol{p})(\breve{\varphi}_1,\breve{\varphi}_2;\psi_1,\psi_2)=\sum_{j=1}^{2}\int_\Omega(\nabla\bar{\psi}_j)^\top[J_p+J_p^\top-(\nabla\cdot\boldsymbol{p})I]\nabla\breve{\varphi}_j,$$
$$g_2(\boldsymbol{p})(\breve{\varphi}_1,\breve{\varphi}_2;\psi_1,\psi_2)=\sum_{j=1}^{2}\kappa_j^2\int_\Omega(\nabla\cdot\boldsymbol{p})\breve{\varphi}_j\bar{\psi}_j.$$

It follows from the well-posedness of the problem (3.16) that [24]

$$\lim_{h\to0}g_k(\boldsymbol{p})(\breve{\varphi}_j,\psi_j)=g_k(\boldsymbol{p})(\varphi_j,\psi_j),\quad k=1,2,\quad j=1,2.$$

Denote

$$\dot{\varphi}_j=\lim_{h\to0}\frac{\breve{\varphi}_j-\varphi_j}{h}.$$

Then we have from (4.6) that

$$a(\dot{\varphi}_1,\dot{\varphi}_2;\psi_1,\psi_2)=g_1(\boldsymbol{p})(\varphi_1,\varphi_2;\psi_1,\psi_2)+g_2(\boldsymbol{p})(\varphi_1,\varphi_2;\psi_1,\psi_2).\tag{4.7}$$

Noting $\boldsymbol{p}=\boldsymbol{0}$ on ∂B and using the identity

$$\begin{aligned}
&(\nabla u)^\top[J_p+J_p^\top-(\nabla\cdot\boldsymbol{p})I]\nabla v\\
=&\nabla\cdot[(\boldsymbol{p}\cdot\nabla u)\nabla v+(\boldsymbol{p}\cdot\nabla v)\nabla u-(\nabla u\cdot\nabla v)\boldsymbol{p}]-(\boldsymbol{p}\cdot\nabla u)\Delta v-(\boldsymbol{p}\cdot\nabla v)\Delta u,
\end{aligned}$$

we get from the divergence theorem that

$$\begin{aligned}
&\int_\Omega (\nabla u)^\top [J_p + J_p^\top - (\nabla\cdot\boldsymbol{p})I]\nabla\bar{v} \\
=&-\int_{\partial D} (\boldsymbol{p}\cdot\nabla u)(\boldsymbol{\nu}\cdot\nabla\bar{v}) + (\boldsymbol{p}\cdot\nabla\bar{v})(\boldsymbol{\nu}\cdot\nabla u) - (\nabla u\cdot\nabla\bar{v})(\boldsymbol{p}\cdot\boldsymbol{\nu}) \\
&-\int_\Omega (\boldsymbol{p}\cdot\nabla u)\Delta\bar{v} - \int_\Omega (\boldsymbol{p}\cdot\nabla\bar{v})\Delta u \\
=&-\int_{\partial D} (\boldsymbol{p}\cdot\nabla\bar{v})(\boldsymbol{\nu}\cdot\nabla u) - (\nabla u\cdot\nabla\bar{v})(\boldsymbol{p}\cdot\boldsymbol{\nu}) \\
&-\int_\Omega (\boldsymbol{p}\cdot\nabla\bar{v})\Delta u + \int_\Omega \nabla(\boldsymbol{p}\cdot\nabla u)\cdot\nabla\bar{v}.
\end{aligned}$$

Lemma 4.2. *Let $\boldsymbol{p}=(p_1,p_2)^\top$ and $\boldsymbol{\nu}=(\nu_1,\nu_2)^\top$ be the unit normal vector on ∂D. Then*

$$\int_{\partial D} (\boldsymbol{p}\cdot\nabla\bar{v})(\boldsymbol{\nu}\cdot\nabla u) - (\nabla u\cdot\nabla\bar{v})(\boldsymbol{p}\cdot\boldsymbol{\nu}) = \int_{\partial D} \boldsymbol{\nu}\cdot\begin{pmatrix} -\partial_y(p_2\partial_x u - p_1\partial_y u) \\ \partial_x(p_2\partial_x u - p_1\partial_y u)\end{pmatrix}\bar{v}.$$

Proof. A simple calculation yields that

$$\begin{aligned}
&\int_{\partial D} (\boldsymbol{p}\cdot\nabla\bar{v})(\boldsymbol{\nu}\cdot\nabla u) - (\nabla u\cdot\nabla\bar{v})(\boldsymbol{p}\cdot\boldsymbol{\nu}) \\
=&\int_{\partial D} (p_1\partial_x\bar{v} + p_2\partial_y\bar{v})(\nu_1\partial_x u + \nu_2\partial_y u) - (\partial_x u\partial_x\bar{v} + \partial_y u\partial_y\bar{v})(p_1\nu_1 + p_2\nu_2) \\
=&\int_{\partial D} \nu_1[p_1\partial_x\bar{v}\partial_x u + p_2\partial_y\bar{v}\partial_x u - p_1\partial_x u\partial_x\bar{v} - p_1\partial_y u\partial_y\bar{v}] \\
&\quad + \nu_2[p_1\partial_x\bar{v}\partial_y u + p_2\partial_y\bar{v}\partial_y u - p_2\partial_x u\partial_x\bar{v} - p_2\partial_y u\partial_y\bar{v}] \\
=&\int_{\partial D} \big(\nu_1\partial_y\bar{v} - \nu_2\partial_x\bar{v}\big)\big(p_2\partial_x u - p_1\partial_y u\big).
\end{aligned}$$

It follows from the divergence theorem that

$$\begin{aligned}
&\int_{\partial D} \big(\nu_1\partial_y\bar{v} - \nu_2\partial_x\bar{v}\big)\big(p_2\partial_x u - p_1\partial_y u\big) \\
=&-\int_\Omega (p_2\partial_x u - p_1\partial_y u)\nabla\cdot\begin{pmatrix}\partial_y\bar{v} \\ -\partial_x\bar{v}\end{pmatrix} - \int_\Omega \begin{pmatrix}\partial_y\bar{v} \\ -\partial_x\bar{v}\end{pmatrix}\cdot\begin{pmatrix}\partial_x(p_2\partial_x u - p_1\partial_y u) \\ \partial_y(p_2\partial_x u - p_1\partial_y u)\end{pmatrix} \\
=&-\int_\Omega \begin{pmatrix}\partial_x\bar{v} \\ \partial_y\bar{v}\end{pmatrix}\cdot\begin{pmatrix}-\partial_y(p_2\partial_x u - p_1\partial_y u) \\ \partial_x(p_2\partial_x u - p_1\partial_y u)\end{pmatrix} \\
=&\int_\Omega \nabla\cdot\begin{pmatrix}-\partial_y(p_2\partial_x u - p_1\partial_y u) \\ \partial_x(p_2\partial_x u - p_1\partial_y u)\end{pmatrix}\bar{v} + \int_{\partial D} \boldsymbol{\nu}\cdot\begin{pmatrix}-\partial_y(p_2\partial_x u - p_1\partial_y u) \\ \partial_x(p_2\partial_x u - p_1\partial_y u)\end{pmatrix}\bar{v} \\
=&\int_{\partial D} \boldsymbol{\nu}\cdot\begin{pmatrix}-\partial_y(p_2\partial_x u - p_1\partial_y u) \\ \partial_x(p_2\partial_x u - p_1\partial_y u)\end{pmatrix}\bar{v},
\end{aligned}$$

which completes the proof. □

Lemma 4.3. *Let $\boldsymbol{\nu}$ and $\boldsymbol{\tau}$ be the unit norm and tangent vectors on ∂D, respectively. Then*

$$\int_{\partial D}(\boldsymbol{p}\cdot\nabla\bar{\psi}_1)(\boldsymbol{\nu}\cdot\nabla\varphi_1)-(\nabla\varphi_1\cdot\nabla\bar{\psi}_1)(\boldsymbol{p}\cdot\boldsymbol{\nu})=\int_{\partial D}\partial_\tau(\boldsymbol{p}\cdot\nabla\varphi_2)\bar{\psi}_1, \tag{4.8}$$

$$\int_{\partial D}(\boldsymbol{p}\cdot\nabla\bar{\psi}_2)(\boldsymbol{\nu}\cdot\nabla\varphi_2)-(\nabla\varphi_2\cdot\nabla\bar{\psi}_2)(\boldsymbol{p}\cdot\boldsymbol{\nu})=-\int_{\partial D}\partial_\tau(\boldsymbol{p}\cdot\nabla\varphi_1)\bar{\psi}_2. \tag{4.9}$$

Proof. Since the proofs of (4.8) and (4.9) are similar, we only show the proof of (4.8). By Lemma 4.2, it suffices to prove

$$\int_{\partial D}\partial_\tau(\boldsymbol{p}\cdot\nabla\varphi_2)\bar{\psi}_1=\int_{\partial D}\boldsymbol{\nu}\cdot\begin{pmatrix}-\partial_y(p_2\partial_x\varphi_1-p_1\partial_y\varphi_1)\\ \partial_x(p_2\partial_x\varphi_1-p_1\partial_y\varphi_1)\end{pmatrix}\bar{\psi}_1.$$

Recalling the boundary condition (3.16)

$$\partial_\nu\varphi_1+\partial_\tau\varphi_2=0,\quad \partial_\nu\varphi_2-\partial_\tau\varphi_1=0$$

and

$$\tau_1=-\nu_2,\quad \tau_2=\nu_1,$$

we get

$$\begin{aligned}(\nu_1\partial_x\varphi_1+\nu_2\partial_y\varphi_1)+(-\nu_2\partial_x\varphi_2+\nu_1\partial_y\varphi_2)=0,\\ (\nu_1\partial_x\varphi_2+\nu_2\partial_y\varphi_2)-(-\nu_2\partial_x\varphi_1+\nu_1\partial_y\varphi_1)=0,\end{aligned}$$

which gives

$$\partial_x\varphi_1=-\partial_y\varphi_2,\quad \partial_y\varphi_1=\partial_x\varphi_2.$$

A simple calculation yields that

$$\begin{aligned}&\int_{\partial D}\boldsymbol{\nu}\cdot\begin{pmatrix}-\partial_y(p_2\partial_x\varphi_1-p_1\partial_y\varphi_1)\\ \partial_x(p_2\partial_x\varphi_1-p_1\partial_y\varphi_1)\end{pmatrix}\bar{\psi}_1\\ =&\int_{\partial D}\boldsymbol{\nu}\cdot\begin{pmatrix}-\partial_y(-p_2\partial_y\varphi_2-p_1\partial_x\varphi_2)\\ \partial_x(-p_2\partial_y\varphi_2-p_1\partial_x\varphi_2)\end{pmatrix}\bar{\psi}_1\\ =&\int_{\partial D}\begin{pmatrix}\nu_1\\ \nu_2\end{pmatrix}\cdot\begin{pmatrix}\partial_y(p_2\partial_y\varphi_2+p_1\partial_x\varphi_2)\\ -\partial_x(p_2\partial_y\varphi_2+p_1\partial_x\varphi_2)\end{pmatrix}\bar{\psi}_1\\ =&\int_{\partial D}\begin{pmatrix}-\nu_2\\ \nu_1\end{pmatrix}\cdot\begin{pmatrix}\partial_x(p_2\partial_y\varphi_2+p_1\partial_x\varphi_2)\\ \partial_y(p_2\partial_y\varphi_2+p_1\partial_x\varphi_2)\end{pmatrix}\bar{\psi}_1\\ =&\int_{\partial D}(\boldsymbol{\tau}\cdot\nabla(\boldsymbol{p}\cdot\nabla\varphi_2))\bar{\psi}_1=\int_{\partial D}\partial_\tau(\boldsymbol{p}\cdot\nabla\varphi_2)\bar{\psi}_1,\end{aligned}$$

which completes the proof. □

Lemma 4.4. *Let $\Delta u+\kappa^2u=0$ in Ω. Then*

$$\kappa^2\int_\Omega(\nabla\cdot\boldsymbol{p})u\bar{v}=-\kappa^2\int_{\partial D}(\boldsymbol{p}\cdot\boldsymbol{\nu})u\bar{v}-\kappa^2\int_\Omega(\boldsymbol{p}\cdot\nabla u)\bar{v}+\int_\Omega(\boldsymbol{p}\cdot\nabla\bar{v})\Delta u.$$

Proof. Using the identity

$$u\bar{v}\nabla\cdot\boldsymbol{p}=\nabla\cdot(u\bar{v}\boldsymbol{p})-(\boldsymbol{p}\cdot\nabla u)\bar{v}-u(\boldsymbol{p}\cdot\nabla\bar{v}),$$

we have from the divergence theorem that

$$\begin{aligned}-\kappa^2\int_{\partial D}(\boldsymbol{p}\cdot\boldsymbol{\nu})u\bar{v}&=-\kappa^2\int_{\partial D}\boldsymbol{\nu}\cdot(\boldsymbol{p}u\bar{v})=\kappa^2\int_{\Omega}\nabla\cdot(\boldsymbol{p}u\bar{v})\\&=\kappa^2\int_{\Omega}u\bar{v}\nabla\cdot\boldsymbol{p}+\kappa^2\int_{\Omega}(\nabla u\cdot\boldsymbol{p})\bar{v}+\kappa^2\int_{\Omega}u(\nabla\bar{v}\cdot\boldsymbol{p})\\&=\kappa^2\int_{\Omega}u\bar{v}\nabla\cdot\boldsymbol{p}+\kappa^2\int_{\Omega}(\nabla u\cdot\boldsymbol{p})\bar{v}-\int_{\Omega}\Delta u(\nabla\bar{v}\cdot\boldsymbol{p}),\end{aligned}$$

which completes the proof. □

Theorem 4.2. *Let (φ_1,φ_2) be the solution of the coupled boundary value problem* (3.16). *Given $p\in C^2(\partial D)^2$, the domain derivative of the scattering operator $\mathscr{S}_j$ is $\mathscr{S}_j'(\partial D,\boldsymbol{p})=\gamma\varphi_j'$, $j=1,2$, where (φ_1',φ_2') is the unique weak solution of the boundary value problem:*

$$\begin{cases}\Delta\varphi_j'+\kappa_j^2\varphi_j'=0 & \text{in } \Omega,\\ \partial_\nu\varphi_1'+\partial_\tau\varphi_2'=\kappa_1^2(\boldsymbol{p}\cdot\boldsymbol{\nu})\varphi_1,\quad \partial_\nu\varphi_2'-\partial_\tau\varphi_1'=\kappa_2^2(\boldsymbol{p}\cdot\boldsymbol{\nu})\varphi_2 & \text{on } \partial D,\\ \partial_\rho\varphi_j'-\mathscr{T}_j\varphi_j'=0 & \text{on } \partial B.\end{cases}\tag{4.10}$$

Proof. Using Lemmas 4.3 and 4.4, we obtain from (4.7) that

$$\begin{aligned}a(\dot{\varphi}_1,\dot{\varphi}_2;\psi_1,\psi_2)&=g_1(\boldsymbol{p})(\varphi_1,\varphi_2;\psi_1,\psi_2)+g_2(\boldsymbol{p})(\varphi_1,\varphi_2;\psi_1,\psi_2)\\&=\sum_{j=1}^{2}\int_{\Omega}(\nabla\bar{\psi}_j)^\top[J_p+J_p^\top-(\nabla\cdot\boldsymbol{p})I]\nabla\varphi_j+\kappa_j^2\int_{\Omega}(\nabla\cdot\boldsymbol{p})\varphi_j\bar{\psi}_j\\&=\sum_{j=1}^{2}\int_{\Omega}\nabla(\boldsymbol{p}\cdot\nabla\varphi_j)\cdot\nabla\bar{\psi}_j-\kappa_j^2\int_{\partial D}(\boldsymbol{p}\cdot\nu)\varphi_j\bar{\psi}_j-\kappa_j^2\int_{\Omega}(\boldsymbol{p}\cdot\nabla\varphi_j)\bar{\psi}_j\\&\quad-\int_{\partial D}\partial_\tau(\boldsymbol{p}\cdot\nabla\varphi_2)\bar{\psi}_1+\int_{\partial D}\partial_\tau(\boldsymbol{p}\cdot\nabla\varphi_1)\bar{\psi}_2.\end{aligned}$$

It is clear that note that $\boldsymbol{p}\cdot\nabla\varphi_j=0$ on ∂B since $\boldsymbol{p}=\boldsymbol{0}$ on ∂B. It follows from (3.15) that

$$\begin{aligned}a(p\cdot\nabla\varphi_1,\boldsymbol{p}\cdot\nabla\varphi_2;\psi_1,\psi_2)=&\sum_{j=1}^{2}\int_{\Omega}\nabla(\boldsymbol{p}\cdot\nabla\varphi_j)\cdot\nabla\bar{\psi}_j-\kappa_j^2\int_{\Omega}(\nabla\varphi_j\cdot\boldsymbol{p})\bar{\psi}_j\\&-\int_{\partial D}\partial_\tau(\boldsymbol{p}\cdot\nabla\varphi_2)\bar{\psi}_1+\int_{\partial D}\partial_\tau(\boldsymbol{p}\cdot\nabla\varphi_1)\bar{\psi}_2.\end{aligned}$$

Denote $\varphi_j'=\dot{\varphi}_j-\boldsymbol{p}\cdot\nabla\varphi_j$, $j=1,2$. We obtain from the above equations that

$$a(\varphi_1',\varphi_2';\psi_1,\psi_2)=-\sum_{j=1}^{2}\kappa_j^2\int_{\partial D}(\boldsymbol{p}\cdot\boldsymbol{\nu})\varphi_j\bar{\psi}_j,$$

which implies that (φ_1',φ_2') satisfies the problem (4.10) and completes the proof. □

4.3 Helmholtz decomposition of the domain derivative

In this subsection, we consider the Helmholtz decomposition of the domain derivative $\boldsymbol{u}'$ for the boundary value problem (4.1), and show that the scalar potentials for the decomposition are the domain derivative for the boundary value problem (4.10).

Theorem 4.3. *Let $\boldsymbol{u}'$ be the solution of the boundary value problem* (4.1)*. Assume that $\boldsymbol{u}'$ admits the following Helmholtz decomposition*

$$\boldsymbol{u}'=\nabla\tilde{\varphi}_1'+\mathbf{curl}\tilde{\varphi}_2',$$

then $(\tilde{\varphi}_1',\tilde{\varphi}_2')$ satisfies (4.10)*, i.e., $\tilde{\varphi}_j'=\varphi_j$, $j=1,2$.*

Proof. Since $\tau_1=-\nu_2$, $\tau_2=\nu_1$, we have

$$\partial_\nu\tilde{\varphi}_j'=\nu_1\partial_x\tilde{\varphi}_j'+\nu_2\partial_y\tilde{\varphi}_j',\quad \partial_\tau\tilde{\varphi}_j'=-\nu_2\partial_x\tilde{\varphi}_j'+\nu_1\partial_y\tilde{\varphi}_j'.$$

By the Helmholtz decomposition

$$\boldsymbol{u}'=\nabla\tilde{\varphi}_1'+\mathbf{curl}\tilde{\varphi}_2'=\begin{pmatrix}\partial_x\tilde{\varphi}_1'+\partial_y\tilde{\varphi}_2'\\ \partial_y\tilde{\varphi}_1'-\partial_x\tilde{\varphi}_2'\end{pmatrix},$$

we may easily verify that $(\tilde{\varphi}_1',\tilde{\varphi}_2')$ satisfies

$$\begin{cases}\Delta\tilde{\varphi}_j'+\kappa_j^2\tilde{\varphi}_j'=0 & \text{in } \Omega,\\ \partial_\rho\tilde{\varphi}_j'-\mathscr{T}_j\tilde{\varphi}_j'=0 & \text{on } \partial B.\end{cases}$$

Hence it only remains to show that

$$\partial_\nu\tilde{\varphi}_1'+\partial_\tau\tilde{\varphi}_2'=\kappa_1^2(\boldsymbol{p}\cdot\boldsymbol{\nu})\varphi_1,\quad \partial_\nu\tilde{\varphi}_2'-\partial_\tau\tilde{\varphi}_1'=\kappa_2^2(\boldsymbol{p}\cdot\boldsymbol{\nu})\varphi_2\quad \text{on } \partial D.$$

We only show the proof for the first equation since the proof is similar for the second equation.

Recalling the Helmholtz decomposition

$$\boldsymbol{u}=\begin{pmatrix}u_1\\ u_2\end{pmatrix}=\nabla\varphi_1+\mathbf{curl}\varphi_2=\begin{pmatrix}\partial_x\varphi_1+\partial_y\varphi_2\\ \partial_y\varphi_1-\partial_x\varphi_2\end{pmatrix},$$

we get

$$\begin{aligned}\nabla\boldsymbol{u}&=\begin{bmatrix}\partial_x u_1 & \partial_y u_1\\ \partial_x u_2 & \partial_y u_2\end{bmatrix}=\begin{bmatrix}\partial_x(\partial_x\varphi_1+\partial_y\varphi_2) & \partial_y(\partial_x\varphi_1+\partial_y\varphi_2)\\ \partial_x(\partial_y\varphi_1-\partial_x\varphi_2) & \partial_y(\partial_y\varphi_1-\partial_x\varphi_2)\end{bmatrix}\\ &=\begin{bmatrix}\partial_{xx}^2\varphi_1+\partial_{xy}^2\varphi_2 & \partial_{xy}^2\varphi_1+\partial_{yy}^2\varphi_2\\ \partial_{xy}^2\varphi_1-\partial_{xx}^2\varphi_2 & \partial_{yy}^2\varphi_1-\partial_{xy}^2\varphi_2\end{bmatrix}.\end{aligned}$$

Hence

$$\partial_\nu \boldsymbol{u} = \boldsymbol{\nu}\cdot\nabla\boldsymbol{u} = \begin{pmatrix} \nu_1\partial^2_{xx}\varphi_1+\nu_1\partial^2_{xy}\varphi_2+\nu_2\partial^2_{xy}\varphi_1+\nu_2\partial^2_{yy}\varphi_2 \\ \nu_1\partial^2_{xy}\varphi_1-\nu_1\partial^2_{xx}\varphi_2+\nu_2\partial^2_{yy}\varphi_1-\nu_2\partial^2_{xy}\varphi_2 \end{pmatrix}.$$

It follows from straightforward calculations that

$$\begin{aligned} \boldsymbol{\nu}\cdot\boldsymbol{u}' &= \boldsymbol{\nu}\cdot(\nabla\tilde{\varphi}_1'+\mathbf{curl}\tilde{\varphi}_2') \\ &= \nu_1(\partial_x\tilde{\varphi}_1'+\partial_y\tilde{\varphi}_2')+\nu_2(\partial_y\tilde{\varphi}_1'-\partial_x\tilde{\varphi}_2') \\ &= (\nu_1\partial_x\tilde{\varphi}_1'+\nu_2\partial_y\tilde{\varphi}_1')-(\nu_2\partial_x\tilde{\varphi}_2'-\nu_1\partial_y\tilde{\varphi}_2') \\ &= \partial_\nu\tilde{\varphi}_1'+\partial_\tau\tilde{\varphi}_2' \end{aligned}$$

and

$$\begin{aligned} \boldsymbol{\nu}\cdot\partial_\nu\boldsymbol{u} =& \nu_1(\nu_1\partial^2_{xx}\varphi_1+\nu_1\partial^2_{xy}\varphi_2+\nu_2\partial^2_{xy}\varphi_1+\nu_2\partial^2_{yy}\varphi_2) \\ &+\nu_2(\nu_1\partial^2_{xy}\varphi_1-\nu_1\partial^2_{xx}\varphi_2+\nu_2\partial^2_{yy}\varphi_1-\nu_2\partial^2_{xy}\varphi_2 \\ =& \nu_1^2\partial^2_{xx}\varphi_1+\nu_1^2\partial^2_{xy}\varphi_2+\nu_1\nu_2\partial^2_{xy}\varphi_1+\nu_1\nu_2\partial^2_{yy}\varphi_2 \\ &+\nu_1\nu_2\partial^2_{xy}\varphi_1-\nu_1\nu_2\partial^2_{xx}\varphi_2+\nu_2^2\partial^2_{yy}\varphi_1-\nu_2^2\partial^2_{xy}\varphi_2. \end{aligned} \tag{4.11}$$

Since $\boldsymbol{u}=0$ on ∂D, we have $\partial_\tau\boldsymbol{u}=0$ and

$$\partial_\tau\boldsymbol{u} = \boldsymbol{\tau}\cdot\nabla\boldsymbol{u} = \begin{pmatrix} -\nu_2 \\ \nu_1 \end{pmatrix}\cdot\begin{bmatrix} \partial^2_{xx}\varphi_1+\partial^2_{xy}\varphi_2 & \partial^2_{xy}\varphi_1+\partial^2_{yy}\varphi_2 \\ \partial^2_{xy}\varphi_1-\partial^2_{xx}\varphi_2 & \partial^2_{yy}\varphi_1-\partial^2_{xy}\varphi_2 \end{bmatrix} = 0,$$

which yields that

$$\begin{aligned} 0 = \boldsymbol{\tau}\cdot\partial_\tau\boldsymbol{u} =& \begin{pmatrix} -\nu_2 \\ \nu_1 \end{pmatrix}\cdot\begin{pmatrix} -\nu_2\partial^2_{xx}\varphi_1-\nu_2\partial^2_{xy}\varphi_2+\nu_1\partial^2_{xy}\varphi_1+\nu_1\partial^2_{yy}\varphi_2 \\ -\nu_2\partial^2_{xy}\varphi_1+\nu_2\partial^2_{xx}\varphi_2+\nu_1\partial^2_{yy}\varphi_1-\nu_1\partial^2_{xy}\varphi_2 \end{pmatrix} \\ =& \nu_2^2\partial^2_{xx}\varphi_1+\nu_2^2\partial^2_{xy}\varphi_2-\nu_1\nu_2\partial^2_{xy}\varphi_1-\nu_1\nu_2\partial^2_{yy}\varphi_2 \\ &-\nu_1\nu_2\partial^2_{xy}\varphi_1+\nu_1\nu_2\partial^2_{xx}\varphi_2+\nu_1^2\partial^2_{yy}\varphi_1-\nu_1^2\partial^2_{xy}\varphi_2. \end{aligned} \tag{4.12}$$

Combining (4.11) and (4.12), we obtain

$$\begin{aligned} \boldsymbol{\nu}\cdot\partial_\nu\boldsymbol{u}+\boldsymbol{\tau}\cdot\partial_\tau\boldsymbol{u} =& \nu_1^2\partial^2_{xx}\varphi_1+\nu_1^2\partial^2_{xy}\varphi_2+\nu_1\nu_2\partial^2_{xy}\varphi_1+\nu_1\nu_2\partial^2_{yy}\varphi_2 \\ &+\nu_1\nu_2\partial^2_{xy}\varphi_1-\nu_1\nu_2\partial^2_{xx}\varphi_2+\nu_2^2\partial^2_{yy}\varphi_1-\nu_2^2\partial^2_{xy}\varphi_2 \\ &+\nu_2^2\partial^2_{xx}\varphi_1+\nu_2^2\partial^2_{xy}\varphi_2-\nu_1\nu_2\partial^2_{xy}\varphi_1-\nu_1\nu_2\partial^2_{yy}\varphi_2 \\ &-\nu_1\nu_2\partial^2_{xy}\varphi_1+\nu_1\nu_2\partial^2_{xx}\varphi_2+\nu_1^2\partial^2_{yy}\varphi_1-\nu_1^2\partial^2_{xy}\varphi_2 \\ =& \partial^2_{xx}\varphi_1+\partial^2_{yy}\varphi_1 = \Delta\varphi_1 = -\kappa_1^2\varphi_1. \end{aligned} \tag{4.13}$$

Using the boundary condition

$$\boldsymbol{u}' = -(\boldsymbol{p}\cdot\boldsymbol{\nu})\partial_\nu\boldsymbol{u} \quad \text{on } \partial D,$$

we have from (4.13) that

$$\begin{aligned}\partial_\nu \tilde{\varphi}_1' + \partial_\tau \tilde{\varphi}_2' = \boldsymbol{\nu}\cdot\boldsymbol{u}' &= -(\boldsymbol{p}\cdot\boldsymbol{\nu})(\boldsymbol{\nu}\cdot\partial_\nu \boldsymbol{u}) \\ &= -(\boldsymbol{p}\cdot\boldsymbol{\nu})(\boldsymbol{\nu}\cdot\partial_\nu \boldsymbol{u} + \boldsymbol{\tau}\cdot\partial_\tau \boldsymbol{u}) = \kappa_1^2(\boldsymbol{p}\cdot\boldsymbol{\nu})\varphi_1.\end{aligned}$$

For similar process $\partial_\nu \tilde{\varphi}_2' - \partial_\tau \tilde{\varphi}_1' = \kappa_2^2(\boldsymbol{p}\cdot\boldsymbol{\nu})\varphi_2$ can be obtained, which completes the proof. □

Remark 4.1. In (4.13), $\Delta\varphi_1 = -k_1^2\varphi_1$ is used on ∂D, which means higher order continuity of φ_1 on ∂D is required.

5 Reconstruction method

In this section, we introduce a numerical method to reconstruct obstacle's surface based on the decomposed system (2.4).

Assume that the obstacle's surface has a parametric equation

$$\partial D = \{\boldsymbol{r} \in \mathbb{R}^2 : \boldsymbol{r}(t) = (r_1(t), r_2(t))^\top,\ t \in [0, 2\pi]\},$$

where r_1, r_2 are twice continuously differentiable and 2π-periodic functions. They admit the following Fourier series expansions

$$r_j(t) = r_j^{(0)} + \sum_{n=1}^{\infty} (r_j^{(2n-1)} \cos(nt) + r_j^{(2n)} \sin(nt)).$$

To reconstruct the surface, it suffices to determine the Fourier coefficients $r_j^{(n)}$. In practice, a cut-off approximation is taken

$$r_{j,N}(t) = r_j^{(0)} + \sum_{n=1}^{N} (r_j^{(2n-1)} \cos(nt) + r_j^{(2n)} \sin(nt)).$$

For large N, $r_{j,N}$ differ from r_j in high frequency modes which represent small details of the obstacle's surface.

Denote by D_N the obstacle with boundary ∂D_N, which has a parametric form

$$\partial D_N = \{r_N(t) \in \mathbb{R}^2 : r_N(t) = (r_{1,N}(t), r_{2,N}(t))^\top,\ t \in [0, 2\pi]\}.$$

Let $\Omega_N = B \setminus \bar{D}_N$. Denote a vector of Fourier coefficients by

$$\mathbf{C} = (c_1, c_2, \cdots, c_{4N+2})^\top \in \mathbb{R}^{4N+2},$$

where $c_{2n+1} = r_1^{(n)}$, $c_{2n+2} = r_2^{(n)}$, $n = 0, 1, \cdots, 2N$, and denote the scattering data for the scalar potential functions from the total field by

$$\boldsymbol{U} = ((\phi_1(x_1), \phi_2(x_1)), \cdots, (\phi_1(x_M), \phi_2(x_M)))^\top \in \mathbb{C}^{2M},$$

where $x_m \in \partial B$, $m=1,\cdots,M$.

There are two different ways to reconstruct obstacle's surface: one is directly from the elastic wave equation (3.12) which has been discussed in [24]; another is from the Helmholtz decomposition (2.4).

The inverse problem can be formulated to solve an approximate nonlinear equation

$$\mathscr{F}_N(\boldsymbol{C})=\boldsymbol{U}.$$

The operator $\mathscr{F}_N$ maps a vector of Fourier coefficients in $\mathbb{R}^{4N+2}$ for the boundary ∂D_N into another vector of scattering data in $\mathbb{C}^{2M}$ for the boundary ∂B.

Theorem 5.1. *Let (φ_1,φ_2) be solution of the problem* (3.16) *corresponding to the obstacle D_N. Then the operator $\mathscr{F}_N$ is differentiable and its derivatives are given by*

$$\frac{\partial \mathscr{F}_{N,m}(\boldsymbol{C})}{\partial c_n}=(\varphi'_{1n}(x_m),\varphi'_{2n}(x_m)),$$

where $(\varphi'_{1n}(x_m),\varphi'_{2n}(x_m))$ is the unique weak solution of the boundary value problem

$$\begin{cases} \Delta\varphi'_{jn}+\kappa_j^2\varphi'_{jn}=0 & \text{in } \Omega_N, \\ \partial_{\nu_N}\varphi'_{1n}(r_N(t))+\partial_{\tau_N}\varphi'_{2n}(r_N(t))=\kappa_1^2 q_n(t)\varphi_1(r_N(t)) & \text{for } t\in[0,2\pi], \\ \partial_{\nu_N}\varphi'_{2n}(r_N(t))-\partial_{\tau_N}\varphi'_{1n}(r_N(t))=\kappa_2^2 q_n(t)\varphi_2(r_N(t)) & \text{for } t\in[0,2\pi], \\ \partial_\rho\varphi'_{jn}-\mathscr{T}_j\varphi'_{jn}=0 & \text{on } \partial B. \end{cases} \tag{5.1}$$

Here $\boldsymbol{\nu}_N$ and $\boldsymbol{\tau}_N$ are the unit normal and tangent vectors on ∂D_N, respectively,

$$q_1(t)=-\frac{r'_{2,N}(t)}{\sqrt{(r'_{1,N}(t))^2+(r'_{2,N}(t))^2}},\quad q_2(t)=\frac{r'_{1,N}(t)}{\sqrt{(r'_{1,N}(t))^2+(r'_{2,N}(t))^2}}$$

and

$$q_n(t)=\begin{cases} q_1(t)\cos(jt), & n=4j-1, \\ q_2(t)\cos(jt), & n=4j, \\ q_1(t)\sin(jt), & n=4j+1, \\ q_2(t)\sin(jt), & n=4j+2, \end{cases}$$

for $j=1,\cdots,N$.

Proof. Let $\boldsymbol{\nu}_N=(\nu_{1N},\nu_{2N})^\top$. It is clear to note that

$$\nu_{1N}=-\frac{r'_{2,N}(t)}{\sqrt{(r'_{1,N}(t))^2+(r'_{2,N}(t))^2}},\quad \nu_{2N}=\frac{r'_{1,N}(t)}{\sqrt{(r'_{1,N}(t))^2+(r'_{2,N}(t))^2}}.$$

Fix $n\in\{1,\cdots,4N+2\}$ and $m\in\{1,\cdots,M\}$, and let $\{\boldsymbol{e}_1,\cdots,\boldsymbol{e}_{4N+2}\}$ be the set of natural basis vectors in $\mathbb{R}^{4N+2}$. By definition, the domain derivative of the m-th component of the operator $\mathscr{F}_N$ on boundary ∂D along with the direction $\boldsymbol{e}_n$ is written as

$$\mathscr{F}'_{N,m}(\boldsymbol{C},\boldsymbol{e}_n)=\frac{\partial\mathscr{F}_{N,m}(\boldsymbol{C})}{\partial c_n}=\lim_{h\to 0}\frac{\mathscr{F}_{N,m}(\boldsymbol{C}+h\boldsymbol{e}_n)-\mathscr{F}_{N,m}(\boldsymbol{C})}{h}.$$

A direct application of Theorem 4.2 shows that the above limit exists,i.e. $\mathscr{F}'_{N,m}(\boldsymbol{C},\boldsymbol{e}_n)=(\varphi'_{1n}(x_m),\,\varphi'_{2n}(x_m))$ and is the unique weak solution of the boundary value problem (5.1). □

Consider an objective function

$$f(\boldsymbol{C})=\frac{1}{2}||\mathscr{F}_N(\boldsymbol{C})-\boldsymbol{U}||^2=\frac{1}{2}\sum_{m=1}^{M}\|\mathscr{F}_{N,m}(\boldsymbol{C})-(\phi_1(x_m),\phi_2(x_m))\|^2.$$

The inverse problem can be formulated as the minimization problem:

$$\min_{\boldsymbol{C}} f(\boldsymbol{C}),\quad \boldsymbol{C}\in\mathbb{R}^{4N+2}.$$

To apply the descent method, it is necessary to compute the gradient of the objective function. Using Theorem 5.1, we have from a simple calculation that

$$\nabla f(\boldsymbol{C})=\left(\frac{\partial f(\boldsymbol{C})}{\partial c_1},\cdots,\frac{\partial f(\boldsymbol{C})}{\partial c_{4N+2}}\right)^{\top},$$

where

$$\frac{\partial f(\boldsymbol{C})}{\partial c_n}=\mathrm{Re}\sum_{m=1}^{M}(\bar{\mathscr{F}}_{N,m}(\boldsymbol{C})-(\bar{\phi}_1(x_m),\bar{\phi}_2(x_m)))\cdot(\varphi'_{1n}(x_m),\varphi'_{2n}(x_m)).$$

Remark 5.1. In practice, the scattering data of the potential functions $(\phi_1(x_m),\phi_2(x_m))$ can be either directly measured or computed from the elastic wave field $\boldsymbol{v}(x_m)$. In fact, it follows from (3.7) that the Fourier modes of $(\phi_1^{(n)},\phi_2^{(n)})$ can be computed from the Fourier modes $\boldsymbol{v}^{(n)}$ via the following equation

$$\begin{bmatrix}\phi_1^{(n)}(R)\\ \phi_2^{(n)}(R)\end{bmatrix}=\left(\frac{n^2}{R^2}-\alpha_1^{(n)}\alpha_2^{(n)}\right)^{-1}\begin{bmatrix}-\alpha_2^{(n)} & -\frac{\mathrm{i}n}{R}\\ -\frac{\mathrm{i}n}{R} & \alpha_1^{(n)}\end{bmatrix}\boldsymbol{v}^{(n)}(R). \tag{5.2}$$

We assume that the scattering data $\mathbf{U}$ is available for a range of frequencies $\omega\in[\omega_{\min},\omega_{\max}]$, which may be divided into $\omega_{\min}=\omega_0<\omega_1<\cdots<\omega_K=\omega_{\max}$. Correspondingly, the compressional wavenumber may be divided into $\kappa_{1,\min}=\kappa_{1,0}<\kappa_{1,1}<\cdots<\kappa_{1,K}=\kappa_{1,\max}$ and the shear wavenumber may be divided into $\kappa_{2,\min}=\kappa_{2,0}<\kappa_{2,1}<\cdots<\kappa_{2,K}=\kappa_{2,\max}$. Let $k_i=[\kappa_{1,i}]$ or $k_i=[\kappa_{2,i}]$, $i=0,1,\cdots,K$ be the greatest integer less than or equal to $\kappa_{1,i}$ or $\kappa_{2,i}$. We now propose an algorithm to reconstruct the Fourier coefficients c_n, $n=1,\cdots,4N+2$.

1. Set an initial approximation $c_3 = c_6 = R_0 > 0$ and $c_n = 0$ otherwise, i.e., the initial approximation is a circle with radius R_0.

2. Begin with the smallest frequency ω_0, and seek an approximation to the functions $r_{j,N}$ by Fourier series with Fourier modes not exceeding k_0:

$$r_{j,k_0} = r_j^{(0)} + \sum_{n=1}^{k_0} (r_j^{(2n-1)} \cos(nt) + r_j^{(2n)} \sin(nt)).$$

   Denote $\mathbf{C}_{k_0} = (c_1, c_2, \cdots, c_{4k_0+2})^\top$ and consider the iteration

$$\mathbf{C}_{k_0}^{(l+1)} = \mathbf{C}_{k_0}^{(l)} - \gamma \nabla f(\mathbf{C}_{k_0}^{(l)}), \quad l = 1, \cdots, L,$$

   where $\gamma > 0$ and $L > 0$ are the step size and the total number of iterations for the descent method, respectively.

3. Increase to the next higher frequency ω_1 of the available data. Repeat Step 2 with the previous approximation to $r_{j,N}$ as the starting point. More precisely, approximate $r_{j,N}$ by

$$r_{j,k_1} = \hat{r}_j^{(0)} + \sum_{n=1}^{k_1} (\hat{r}_j^{(2n-1)} \cos(nt) + \hat{r}_j^{(2n)} \sin(nt)),$$

   and determine the coefficients $\hat{c}_n$, $n = 1, 2, \cdots, 4k_1 + 2$ by using the descent method starting from the previous result:

$$\hat{c}_n = \begin{cases} c_n & \text{for } 1 \le n \le 4k_0 + 2, \\ 0 & \text{for } 4k_0 + 2 < n \le 4k_1 + 2, \end{cases}$$

   where the coefficients c_n come from Step 2. The resulting solution in this step represents the Fourier coefficients of $r_{j,N}$ corresponding to the frequencies not exceeding k_1.

4. Repeat Step 3 until a prescribed highest frequency ω_K is reached.

We need to choose the prescribed frequency larger than the highest Fourier mode of the surface in order to get a complete reconstruction. Numerical experiments show that the recursive method converges for a wider class of surfaces than the usual Newton method starting at the same initial guess of a circle with radius R_0.

6 Numerical experiments

In this section, we take the two examples which are adopted in [24] to show the results of the proposed method. The scattered data is obtained from the solution of problem

(3.12) and the formula (5.2) in terms of the Fourier transform. The direct problem (3.12) is solved by the finite element method with the perfectly matched layer technique, which is implemented via FreeFem++ [14]. The finite element solution is interpolated uniformly on ∂B. To test the stability, we add some relative noise to the data

$$\boldsymbol{u}^{\delta}(x_i)=\boldsymbol{u}(x_i)(1+\delta\,\mathrm{rand}),\quad i=1,\cdots,M,$$

where rand are uniformly distributed random numbers in $[-1,1]$. Since the measurement points $x_i\in\partial B$, we have $x_i=(R\cos\psi_i,R\sin\psi_i)^{\top}$, where $\psi_i\in[0,2\pi]$ is the observation angle.

In the following two examples, we take the Lamé constants $\lambda=2$, $\mu=1$, which account for the compressional wavenumber $\kappa_1=\omega/2$ and the shear wavenumber $\kappa_2=\omega$. The radius of the ball B is $R=2.5$ and the radius of the initial guess of the circle $R_0=1.0$. The observation points $M=64$. The noise level $\delta=5\%$.

Example 6.1. Consider a commonly used benchmark test example, a kite-shaped obstacle, which has the parametric equation

$$r_1(t)=-0.65+\cos(t)+0.65\cos(2t),\quad r_2(t)=1.5\sin(t),\quad t\in[0,2\pi].$$

The obstacle's surface has a concave part. It has become a criterion to judge the quality of a reconstruction method whether the concave part of the obstacle can be successfully recovered. Our approach is essentially a Fourier spectral method and aims to recover the Fourier coefficients. Since the surface functions only contain a couple of low Fourier modes, our method works very well even by using few scattering data. Here we use a single compressional plane wave with the incident angle $\theta=0$ to illuminate the obstacle. We take the scattering data at three frequencies $\omega_0=2$, $\omega_1=4$ and $\omega_2=6$, i.e., the compressional wavenumbers are $\kappa_{1,0}=1$, $\kappa_{1,1}=2$, $\kappa_{1,2}=3$. In the iteration process, the step size $\gamma=0.005$, and for each wave number, the total number of iterations $L=10$. Fig. 2(a) shows the exact surface and the initial guess of the unit circle. Fig. 2(b) shows the reconstructed surface by using the full aperture data, i.e., the observation angle $\psi\in[0,2\pi]$. The result is almost perfect. We also investigate how the data aperture influences the quality of the reconstruction. Fig. 2(c)-(i) plot the reconstructed surfaces and the corresponding data apertures for the construction. It is clear to note that the results are as good as the one by using the full aperture data as long as the observation angles cover the concave part of the obstacle; the results deteriorate as the aperture gets smaller if the observation angles don't cover the concave part of the obstacle.

Example 6.2. Consider a star-shaped obstacle, which has the parametric equation

$$\begin{aligned}r_1(t)&=1.5\cos(t)+0.15\cos(4t)+0.15\cos(6t),\\ r_2(t)&=1.5\sin(t)-0.15\sin(4t)+0.15\sin(6t),\end{aligned}$$

where $t\in[0,2\pi]$. Due to the oscillatory feature, this surface contains many more high Fourier modes and is more difficult than the first example. The scattering data with

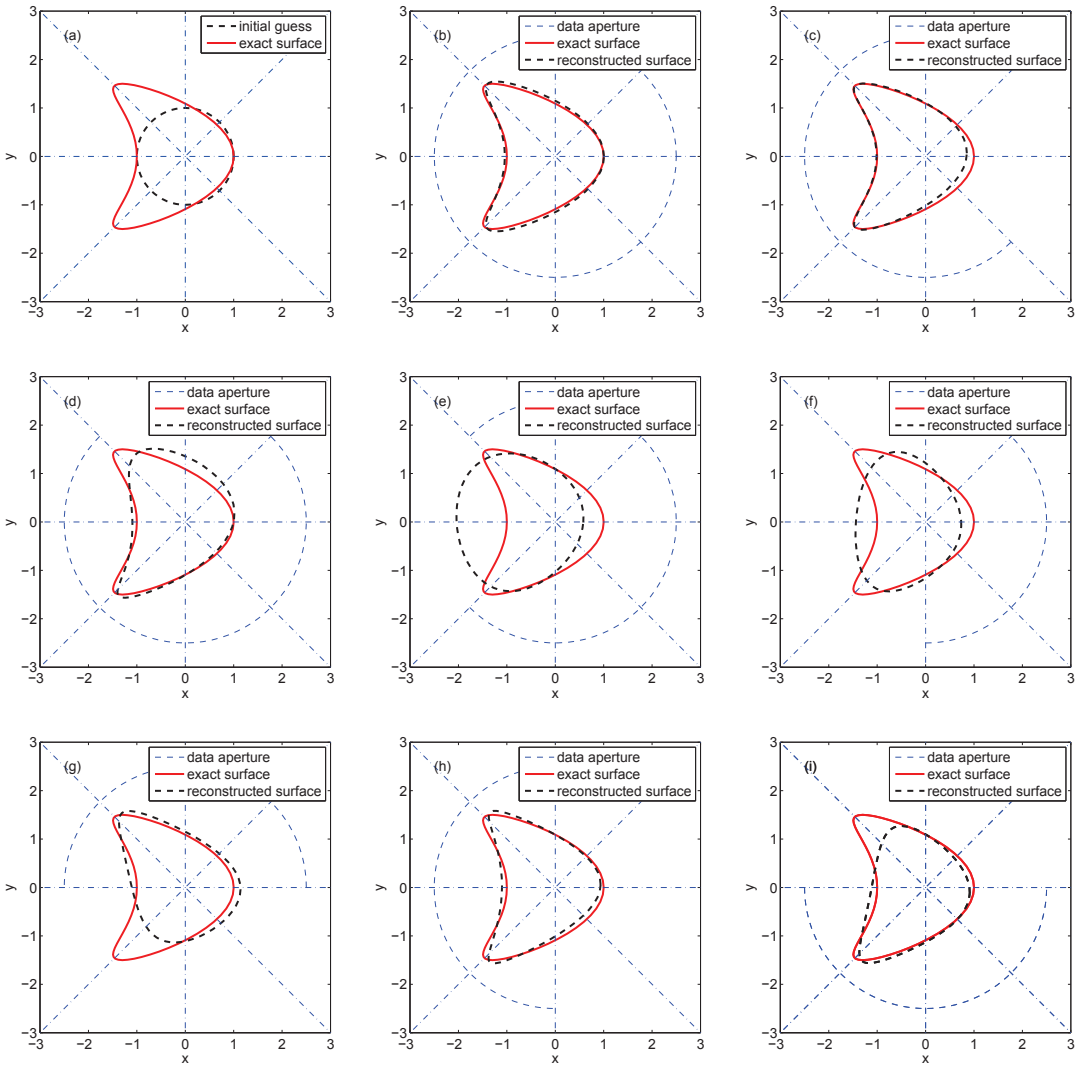

Figure 2: Example 6.1: the kite-shaped obstacle. (a) exact surface and initial guess of the unit circle; (b) $\psi\in[0,2\pi]$; (c) $\psi\in[\frac{\pi}{4},\frac{7\pi}{4}]$; (d) $\psi\in[0,\frac{\pi}{4}]\cup[\frac{3\pi}{4},2\pi]$; (e) $\psi\in[0,\frac{3\pi}{4}]\cup[\frac{5\pi}{4},2\pi]$; (f) $\psi\in[0,\frac{\pi}{2}]\cup[\frac{3\pi}{2},2\pi]$; (g) $\psi\in[0,\pi]$; (h) $\psi\in[\frac{\pi}{2},\frac{3\pi}{2}]$; (i) $\psi\in[\pi,2\pi]$.

higher frequencies is required in order to completely recover the obstacle. In this example, we use a combination of two compressional plane waves with incident angles $\theta=0,\pi$ to illuminate the obstacle. We take the scattering data at four frequencies $\omega_0=2$, $\omega_1=4$, $\omega_2=6$, $\omega_3=8$, i.e., the compressional wavenumbers are $\kappa_{2,0}=1$, $\kappa_{2,1}=2$, $\kappa_{2,3}=3$, $\kappa_{2,4}=4$. In the iterative process, the step size $\gamma=0.005$ and the total number of iterations $L=5$ at each wavenumber. Fig. 3(a) shows the exact surface and the initial guess of the unit circle. Fig. 3(b)-(i) show the reconstructed surfaces by using different data apertures. We can

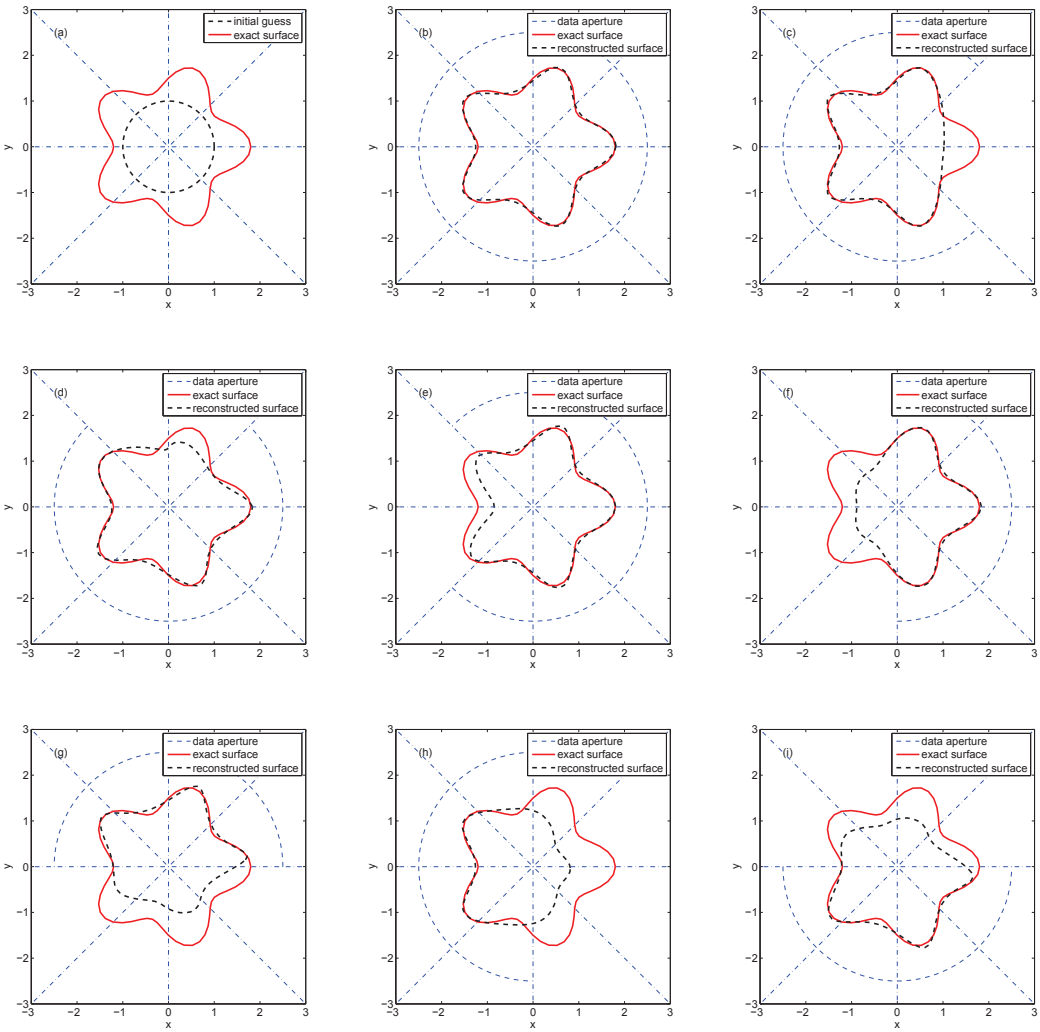

Figure 3: Example 6.2: the star-shaped obstacle. (a) exact surface and initial guess of the unit circle; (b) $\psi\in[0,2\pi]$; (c) $\psi\in[\frac{\pi}{4},\frac{7\pi}{4}]$; (d) $\psi\in[0,\frac{\pi}{4}]\cup[\frac{3\pi}{4},2\pi]$; (e) $\psi\in[0,\frac{3\pi}{4}]\cup[\frac{5\pi}{4},2\pi]$; (f) $\psi\in[0,\frac{\pi}{2}]\cup[\frac{3\pi}{2},2\pi]$; (g) $\psi\in[0,\pi]$; (h) $\psi\in[\frac{\pi}{2},\frac{3\pi}{2}]$; (i) $\psi\in[\pi,2\pi]$.

see that the part of the surface can be accurately reconstructed as long as the observation angles cover that part.

7 Concluding remarks

In this paper, we have studied the inverse obstacle scattering problem for elastic waves in two dimensions. Based on the Helmholtz decomposition and transparent boundary

conditions, the boundary value problem of the Navier equation is converted into a coupled boundary value problem of the Helmholtz equations. The domain derivatives are investigated for the potential functions from two different aspects: one is to deduce the domain derivative from the coupled boundary value problem of the potential functions by using the variational approach; another is to take the Helmholtz decomposition of the domain derivative for the displacement of the original Navier system. We show that the two approaches are consistent and give the same domain derivative for the coupled Helmholtz system. A frequency recursive method is developed for the inverse problem. Numerical examples are presented to demonstrate the effectiveness and stability of the proposed method. The results are comparable to those presented in [24], which requires to solve the Navier equation. This work requires to solve the simpler Helmholtz equation. It provides a viable method to solve the inverse elastic obstacle scattering problem. A possible continuation of this work is to study the three-dimensional problem and different boundary conditions.

Acknowledgments

The research was supported by the National Natural Science Foundation of China (Grant No. 11771321).

References

[1] H. Ammari, E. Bretin, J. Garnier, H. Kang, H. Lee, and A. Wahab, Mathematical Methods in Elasticity Imaging, Princeton University Press, New Jersey, 2015.
[2] G. Bao, G. Hu, J. Sun, and T. Yin, Direct and inverse elastic scattering from anisotropic media, J. Math. Pures Appl., 117(2018), 263–301.
[3] G. Bao, P. Li, J. Lin, and F. Triki, Inverse scattering problems with multi-frequencies, Inverse Probl., 31(2015), 093001.
[4] G. Bao, P. Li, and H. Wu, A computational inverse diffraction grating problem, J. Opt. Soc. Am. A, 29(2012), 394–399.
[5] G. Bao, J. Lv, and P. Li, Numerical solution of an inverse diffraction grating problem from phaseless data, J. Opt. Soc. Am. A, 30(2013), 293–299.
[6] M. Bonnet and A. Constantinescu, Inverse problems in elasticity, Inverse Probl., 21(2005), 1–50
[7] A. Charalambopoulos, On the Fréchet differentiability of the boundary integral operators in the inverse elastic scattering problems, Inverse Probl., 11(1995), 1137–1161.
[8] J. Chen and G. Huang, A Direct Imaging Method for Inverse Electromagnetic Scattering Problem in Rectangular Waveguide, Commun. Comput. Phys., 23(2017), 1415–1433.
[9] R. Coifman, M. Goldberg, T. Hrycak, M. Israeli, and V. Rokhlin, An improved operator expansion algorithm for direct and inverse scattering computations, Waves Random Media, 9(1999), 441–457.
[10] Z. Chen and G. Huang, Phaseless Imaging by Reverse Time Migration: Acoustic Waves, Numer. Math.-Theory Methods Appl., 10(2017),1–21.

[11] J. Elschner and M. Yamamoto, Uniqueness in inverse elastic scattering with nitely many incident waves, Inverse Probl., 26(2010), 045005.
[12] H. Haddar and R. Kress, On the Fréchet derivative for obstacle scattering with an impedance boundary condition, SIAM J. Appl. Math., 65(2004), 194–208.
[13] P. Hahner and G. C. Hsiao, Uniqueness theorems in inverse obstacle scattering of elastic waves, Inverse Probl., 9(1993), 525–534.
[14] F. Hecht, New development in FreeFem++, J. Numer. Math. 20(2012), 251–265.
[15] F. Hettlich, Fréchet derivatives in inverse obstacle scattering, Inverse Probl., 11(1995), 371–382. Erratum: Fréchet derivatives in inverse obstacle scattering, Inverse Probl., 14(1998), 209–210.
[16] G. Hu. A. Kirsch, and M. Sini, Some inverse problems arising from elastic scattering by rigid obstacles, Inverse Probl., 29(2013), 015009.
[17] G. Hu, J. Li, H. Liu, and H. Sun, Inverse elastic scattering for multiscale rigid bodies with a single far-field pattern, SIAM J. Imaging Sci., 7(2014), 1799–1825.
[18] M. Kar and M. Sini, On the inverse elastic scattering by interfaces using one type of scattered waves, J. Elast., 118(2015), 15–38
[19] A. Kirsch, The domain derivative and two applications in inverse scattering theory, Inverse Probl., 9(1993), 81–96.
[20] R. Kress, Inverse elastic scattering from a crack, Inverse Probl., 12(1996), 667–684.
[21] L. D. Landau and E. M. Lifshitz, Theory of Elasticity, Oxford: Pergamon 1986.
[22] F. Le Louër, A domain derivative-based method for solving elastodynamic inverse obstacle scattering problems, Inverse Probl., 31(2015), 115006.
[23] F. Le Louër, On the Fréchet derivative in elastic obstacle scattering SIAM J. Appl. Math., 72(2012), 1493–1507
[24] P. Li, Y. Wang, Z. Wang, and Y. Zhao, Inverse obstacle scattering for elastic waves, Inverse Probl., 32(2016), 115018.
[25] P. Li P, Y. Wang, and Y. Zhao, Inverse elastic surface scattering with near-field data, Inverse Probl., 31(2015), 035009
[26] P. Li and X. Yuan, Inverse obstacle scattering for elastic waves in three dimensions, Inverse Probl., 32(2017), 115018.
[27] G. Nakamura and G. Uhlmann, Inverse problems at the boundary of elastic medium, SIAM J. Math. Anal., 26(1995), 263–279.
[28] R. Potthast, Fréchet differentiability of boundary integral operators in inverse acoustic scattering, Inverse Probl., 10(1994), 431–447.
[29] R. Potthast, Domain derivatives in electromagnetic scattering, Math. Meth. Appl. Sci., 19(1996), 1157–1175.
[30] Sommerfeld, Partial Differential Equations in Physics, Academic Press, New York, New York, 1949.
[31] M. Sini and N. T. Thanh, Inverse acoustic obstacle scattering problems using multifrequency measurements, Inverse Probl. Imaging, 6(2012), 749–773.
[32] Andre Roger, Newton–Kantorovitch algorithm applied to an electromagnetic inverse problem, IEEE Trans. Antennas Propag., 29(1981), 232–238.
[33] M. Zhang and J. Lv, Numerical method of profile reconstruction for a periodic transmission problem from single-sided data, Commun. Computat. Phys., 24(2018), 435–453.